DOE/ET/12229-T1

SOLIDS CIRCULATION AROUND A JET IN A FLUIDIZED BED GASIFIER

Final Technical Report for Period September 1, 1978—September 30, 1980

By
Dimitri Gidaspow
Bozorg Ettehadieh
Chungliang Lin
Anil Goyal
Robert W. Lyczkowski

May 1980

Work Performed Under Contract No. FG21-78ET12229

Illinois Institute of Technology
Chicago, Illinois

U. S. DEPARTMENT OF ENERGY

DISCLAIMER

DISCLAIMER

Available from the National Technical Information Service, U. S. Department of Commerce, Springfield, Virginia 22161.

Price: Printed Copy A05
Microfiche A01

DOE/ET/12229-T1
Distribution Category UC-90c

SOLIDS CIRCULATION AROUND A JET IN A FLUIDIZED BED GASIFIER

ILLINOIS INSTITUTE OF TECHNOLOGY

DOE Grant Number ET-78-G-01-3381
9/1/78 - 9/30/80

FINAL TECHNICAL REPORT

by

Dimitri Gidaspow, Principal Investigator

Bozorg Ettehadieh, Ph.D. Candidate
(computer solution)

Chungliang Lin, MS Candidate
(fluidized bed experiment)

Anil Goyal, Ph.D. May 1980
(entrained flow coal gasification reactor)

and

Robert W. Lyczkowski, Ph.D.
(consultant)

Table of Contents

ABSTRACT

The object of this investigation was to develop an experimentally verified hydrodynamic model to predict solids circulation around a jet in a fluidized bed gasifier. Hydrodynamic models of fluidization use the principles of conservation of mass, momentum and energy. To account for unequal velocities of solid and fluid phases, separate phase momentum balances are developed. Other fluid bed models used in the scale-up of gasifiers do not employ the principles of conservation of momentum. Therefore, these models cannot predict fluid and particle motion. In such models solids mixing is described by means of empirical transfer coefficients.

A two dimensional unsteady state computer code was developed to give gas and solid velocities, void fractions and pressure in a fluid bed with a jet. The growth propagation and collapse of bubbles was calculated. Time averaged void fractions were calculated that showed an agreement with void fractions measured with a gamma ray densitometer. Calculated gas and solid velocities in the jet appeared to be reasonable. Pressure and void oscillations also appear to be reasonable.

A simple analytical formula for the rate of solids circulation was developed from the equations of change. It agrees with Westinghouse fluidization data in a bed with a draft tube. One dimensional hydrodynamic models were applied to modeling of entrained-flow coal gasification reactors and compared with data.

Further development of the hydrodynamic models should make the scale-up and simulation of fluidized bed reactors a reality.

BACKGROUND OF HYDRODYNAMIC MODELS

A hydrodynamic approach to fluidization was started by Davidson in 1961. He analyzed single bubble motion in an infinite fluid bed using two continuity equations and an expression for relative velocities in terms of Darcy's law for flow in porous media. Davidson assumed that the solids flow around a bubble was irrotational. This assumption (Gidaspow and Solbrig, 1976) can be justified based on the mixture momentum equation. It can also be shown (Gidaspow and Solbrig, 1976) that the use of Darcy's law and the mixture momentum equation is in the limit equivalent to the use of two separate phase momentum balances. It is therefore interesting to note here that Davidson's solution of the degenerate equations of motion led to important predictions. He predicted that a spherical surface of zero velocity - called a cloud - will follow the bubble. Shortly after his prediction, the existence of a cloud was verified experimentally by inserting No_X into a bubble. The concept of cloud is so important that one actually denotes it to be a phase in the transfer coefficient models of Levenspiel and others (Wen, 1975; Babu et al., 1976).

A year after Davidson's solution, Jackson (1963) formulated the more general equations of motion. In 1971 Jackson reviewed his work and that of others. Jackson and co-investigators (Anderson and Jackson, 1967 and Medlin, Wong and Jackson, 1974) continued the development of their equations and analysis of hydrodynamic instabilities. In the

1960's and early 1970's there were parallel developments of hydrodynamic equations by several investigators, the better known being by Murry (1965), Pigford and Baron (1965), Soo (1967), Ruckenstein and Tzeculescu (1967). At the 1967 International Fluidization Symposium there was an interesting discussion of various hydrodynamic equations chaired by van Deemter (1967). He showed that all cited authors try to determine the solids velocity, the fluid velocity, the pressure and void fraction. However, he concluded that there was no general agreement about the momentum equations. In these years there was little attempt to numerically solve the equations of change without making radical approximations, such as assuming the void fraction to be constant away from the bubble, as is done by numerous followers of Davidson and Harrison.

In the last few years interest in hydrodynamic modeling was renewed due to the energy crisis (Gidaspow and Solbrig, 1976). When an attempt was made to solve the hydrodynamic models similar to those presented by Jackson numerically on high-speed computers, it was found that the differential equations are ill-posed as an initial value problem (Gidaspow, 1974; Lyczkowski et al., 1978). According to our interpretations of Lax's theorem (Lax, 1958) and the von Neumann linearized stability analysis, it is impossible to find a numerically stable finite difference technique to solve such a set of equations. However, in view of the usually small numerical values of the imaginary

characteristics and the comparatively large numerical damping caused by finite differencing, computer codes such as the K - fix based on the ill-posed equations (Rivard and Torrey, 1976) are able to produce very reasonable results, without using gas and solid stress displacement tensors, with viscosity coefficients whose values are at best, highly questionable today.

An updated review of two-phase flow modeling will appear by Lyczkowski, Gidaspow and Solbrig (1981). While there are many new two-phase flow models, the newer one developed by Soo (1980), only those for which numerical values were obtained for fluidization problems will be discussed below.

The first and earliest approach involves the application of Newton's second law of motion for particles. Added mass forces are neglected. Void fractions are usually assumed to be constant. This restricts the application to dilute systems. Rudinger and Chung (1964) presented one of the first such solutions to transient gas-particle flow. This set of equations is not ill-posed. When the void fraction is allowed to vary, Arastoopour and Gidaspow (1979) showed that such a model produces reasonable results for vertical pneumatic conveying. Scharff, et al., (1980) have generalized Rudinger's approach. The void fraction is not one of the variables in the differential equations, but is calculated based on the size and number of particles in a computational cell. No comparison of the theory to data

has been reported in the open literature by the Department of Energy funded groups.

The second approach involves a modification of Jackson's equations by a Systems, Science and Software group (Pritchett, Blake and Garg, 1978, Garg and Pritchett, 1975; Blake, Brownell and Schneyer, 1979). They showed that these equations can at least qualitatively, predict the motion of a bubble through a fluidized bed. Quantitative comparisons with data have apparently not been made.

The third approach is to derive equations of relative motion using the principles of nonequilibrium thermodynamics. This approach was described by Gidaspow (1978), compared with pneumatic transport data, (Arastoopour and Gidaspow, 1979) and with solids mixing data in fluidized beds (Liu and Gidaspow, 1980). The equations correctly reduce themselves to a generalized form of Fick's law of diffusion and satisfy the material frame indifference principle, as is the case in the by now almost classical treatment of single phase multicomponent mixture theory (Bowen, 1976). They do not as yet include "second order" terms involving gas and solids viscosities and particle to particle interaction associated with a solids pressure. Application of this theory to gas-solids flow was recently reviewed by Leung (1980). The only differential equations given in his review are those of Arastoopour and Gidaspow. This reflects the state-of-the-art of hydrodynamic modeling.

SUMMARY OF RESEARCH PROGRESS TO DATE

Progress made by the author and graduate students in developing a hydrodynamic theory of fluidization is summarized below.

A new theory of pneumatic transport was developed. It is described in the following publications:

(1) H. Arastoopour and D. Gidaspow, "Vertical Countercurrent Solids Gas Flow" Chem. Eng. Science 34, 1063-66 (1979).

(2) H. Arastoopour and D. Gidaspow, "Analysis of IGT Pneumatic Conveying Data and Fast Fluidization Using a Thermohydrodynamic Model" Powder Technology 22, 77-87 (1979).

(3) H. Arastoopour and D. Gidaspow, "Vertical Pneumatic Conveying Using Four Hydrodynamic Models" I&EC Fundamentals 18, 123-130 (1979).

The above theory was favorably reviewed in the recent Fluidization Conference. See L. S. Leung, "The Ups and Downs of Gas-Solid Flow—A Review," in "Fluidization" ed. J. R. Grace and J. M. Matsen; Plenum Press, 1980.

The theory was extended to a mixture of particle sizes and was presented at the 2nd Multi-Phase Flow and Heat Transfer Symposium on April 16-18, 1979. It is published in "Multiphase Transport: Fundamentals, Reactor Safety, Applications" editor, T. N. Veziroglu, Hemisphere Publishing Corp. (1980) under the title "Hydrodynamic Analysis of Pneumatic Transport of a Mixture of Two Particle Sizes" by H. Arastoopour, D. Lin (graduate students at that time) and D. Gidaspow.

A paper by Y. Liu and D. Gidaspow, "Solids Mixing in Fluidized Beds—A Hydrodynamic Approach" was accepted for publication in Chemical Engineering Science.

A paper "Hydrodynamics of Solids Mixing in a Gasifier" was presented at the 1980 International Fluidization Conference in Henniker, New Hampshire. The details of that presentation and subsequent developments are summarized below.

FLUIDIZATION IN A TWO DIMENSIONLESS BED WITH A JET

Hydrodynamic models of fluidization use the principles of conservation of mass, momentum and energy. Figure 1 shows the continuity and mixture momentum equations for two dimensional transient two-phase flow. Figure 2 shows the additional equations needed to determine the velocity components for the gas, Ug, Vg, for the solid U_s, V_s, void fraction, ε and the pressure, P. Two models are being considered. One is a basic ill-posed model for which a computer code, called K-FIX was developed at Los Alamos. This code was modified during the past year under the sponsorship of the Department of Energy grant to apply to fluidization. The second model is the relative velocity model derived using non-equilibrium thermodynamic principles (Gidaspow, 1978). The equations are a generalization of those already studied by Arastoopour and Gidaspow (1979) for pneumatic transport.

In the partial differential equations shown in Figures 1 and 2 β is the friction coefficient, which Soo (1967) calls F in his book.

TWO DIMENSIONAL UNSTEADY HYDRODYNAMIC MODELS

COMMON EQUATIONS

GAS CONTINUITY

$$\frac{\delta}{\delta t}(\rho_g \epsilon) + \frac{\delta}{\delta x}(\epsilon \rho_g u_g) + \frac{\delta}{\delta y}(\epsilon \rho_g v_g) = 0$$

SOLIDS CONTINUITY

$$\frac{\delta}{\delta t}[\rho_s(1-\epsilon)] + \frac{\delta}{\delta x}[\rho_s u_s(1-\epsilon)] + \frac{\delta}{\delta y}[\rho_s v_s(1-\epsilon)] = 0$$

MIXTURE MOMENTUM IN x DIRECTION

$$\epsilon \rho_g \frac{\delta u_g}{\delta t} + \rho_s(1-\epsilon)\frac{\delta u_s}{\delta t} + \epsilon \rho_g\left[u_g \frac{\delta u_g}{\delta x} + v_g \frac{\delta u_g}{\delta y}\right] + \rho_s(1-\epsilon)\left[u_s \frac{\delta u_s}{\delta x} + v_s \frac{\delta u_s}{\delta y}\right] =$$
$$-\frac{\delta P}{\delta x} - g_x[\rho_s(1-\epsilon) + \rho_g \epsilon] - f_{wx}$$

MIXTURE MOMENTUM IN y DIRECTION

$$\epsilon \rho_g \frac{\delta v_g}{\delta t} + \rho_s(1-\epsilon)\frac{\delta v_s}{\delta t} + \epsilon \rho_g\left[v_g \frac{\delta v_g}{\delta y} + u_g \frac{\delta v_g}{\delta x}\right] + \rho_s(1-\epsilon)\left[v_s \frac{\delta v_s}{\delta y} + u_s \frac{\delta v_s}{\delta x}\right] =$$
$$-\frac{\delta P}{\delta y} - g_y[\rho_s(1-\epsilon) + \rho_g \epsilon] - f_{wy}$$

WE WANT TO DETERMINE u_g, v_g, u_s, v_s, ϵ, AND P.
THEREFORE, WE NEED TWO MORE EQUATIONS.

Fig. 1. Conservation of Mass and Mixture Momentum

ILL-POSED AND THERMODYNAMICALLY DERIVED EQUATIONS

THE ADDITIONAL MOMENTUM EQUATIONS FOR EACH MODEL ARE :

CASE A. PRESSURE DROP IN BOTH SOLID AND GAS PHASES (ILL-POSED MODEL)

SOLIDS MOMENTUM IN x DIRECTION

$$\frac{\delta u_s}{\delta t} + u_s \frac{\delta u_s}{\delta x} + v_s \frac{\delta u_s}{\delta y} = -1/\rho_s \frac{\delta P}{\delta x} - g_x + \beta(u_g - u_s)$$

SOLIDS MOMENTUM IN y DIRECTION

$$\frac{\delta v_s}{\delta t} + v_s \frac{\delta v_s}{\delta y} + u_s \frac{\delta v_s}{\delta x} = -1/\rho_s \frac{\delta P}{\delta y} - g_y + \beta(v_g - v_s)$$

CASE B. RELATIVE VELOCITY MODEL (CONSTITUTIVE EQUATION)

x DIRECTION

$$(u_g - u_s)\frac{\delta}{\delta x}(u_g - u_s) + (v_g - v_s)\frac{\delta}{\delta y}(u_g - u_s) - \beta(u_g - u_s) + g_x = 0$$

y DIRECTION

$$(v_g - v_s)\frac{\delta}{\delta y}(v_g - v_s) + (u_g - u_s)\frac{\delta}{\delta x}(v_g - v_s) - \beta(v_g - v_s) + g_y = 0$$

β IS EVALUATED USING AN ERGUN EQUATION FOR $\alpha < 0.8$ AND RICHARDSON AND ZAKI'S EXPRESSION FOR DRAG FOR $\alpha \geq 0.8$

Fig. 2. Conservation of Momentum for the Solid Phase

According to Wen and Yu, (1966) for a particularly fluidized bed of voidage less than 0.8 the friction between the gas and the solid can be described by the Ergun equation:

$$\beta = 150 \frac{(1-\varepsilon)^2 \mu_g}{\varepsilon^2 (d_p \phi_s)^2} + 1.75 \frac{\rho_g (1-\varepsilon)(U_g - U_s)}{\varepsilon (\phi_s d_p)}$$

For porosities greater than 0.8 expressions found by Richardson and Zaki (1954) and Wen and Yu (1966) are used. According to Richardson and Zaki,

$$\beta = \frac{3}{4} C_D \frac{(U_g - U_s)\rho_g (1-\varepsilon)}{(\phi_s d_p)} \varepsilon^n$$

where C_D, the drag coefficient, is related to Reynolds number (Rowe 1961) by the relations:

$$C_D = \frac{24}{Re_s} (1 + .15\ Re_s^{.687}) \qquad Re_{s_x} < 1000$$

$$C_D = 0.44 \qquad Re_{s_x} \geq 1000$$

$$\text{where } Re_{s_x} = \frac{\varepsilon \rho_g (U_g - U_s)}{\mu_g}$$

n shows the effect due to presence of other particles in the emulsion and is also dependent on the relative motion of the solid-gas system.

$$n = 4.65 \qquad .01 < Re_{s_x} \leq 2.$$

$$n = 3.37 \qquad 2 < Re_{s_x} \leq 500$$

$$n = 2.35 \qquad 500 < Re_{s_x}$$

The friction with the walls denoted by fwx and fwy have been tentatively set to zero.

This set of non-linear partial differential equations is solved for U_s, V_s, U_g, V_g, ε and P using the numerics of the K-FIX program (Rivard and Travis, 1977). The boundary conditions used are as follows:

B.C1: At y = 0 we have

$\rho_g V_g = C_1$, that is constant gas mass flux, and also $U_g = 0$, $V_s = 0$, $U_s = 0$, $\varepsilon = 1.0$.

B.C2: at Y=L, we have P = atmospheric and $V_s = 0$ that is a wire mesh to prevent solid carry over from bed.

B.C3: At x = 0 $U_s = U_g = 0$ due to the jet center (solid wall with free slip)

B.C4: At x = W $U_s = U_g = 0$ that is we have a solid wall with no slip
$V_g = 0$

The initial condition is assumed to be that of minimum fluidization.

A free board of the same size as initial bed height is provided to allow for bed expansion. At time zero a jet gas is allowed to enter the bed. Figure 3 shows the bed dimensions, the particle diameter and the other data used in the numerical calculations reported here. For short operation times, of the order of one second real time and corresponding to 15 minutes on the Cray computer reasonable results were obtained with the ill posed model. For longer times material balance could not be maintained. This may be a symptom of the ill-posedness that manifests itself despite the fact that the terms that cause the ill-posedness are very small. The mixing in this bed is essentially driven by

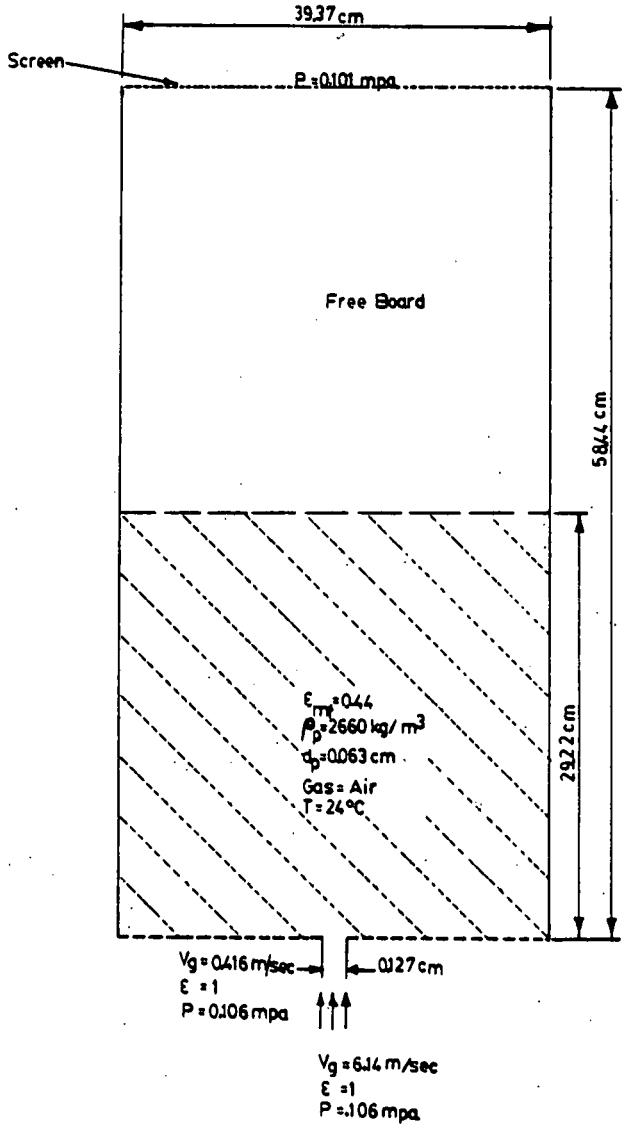

Fig. 3. Data for Numerical Computations

density gradients. An approximate analytical solution to the rate of solids circulation had been found which agreed with Westinghouse data for a draft tube inserted into the fluid bed.

Figure 4 shows the growth and collapse of a bubble in a two-dimensional fluidized bed initially at minimum fluidization. At zero time a jet with a velocity of 6.14 m/sec was turned on. We see the formation of voids, marked as $\varepsilon = 0.9$ and $\varepsilon = 0.96$, their propagation and the collapse of the void or bubble, as observed in the laboratory in a two-dimensional plastic bed.

Figure 5 shows the time averaged computed void fractions in the bed. We see that the maximum void is not near the jet inlet, but a considerable distance into the bed. This is the first time that such profiles were ever computed by anybody for a fluid bed. Figure 6 shows a comparison of these results to experimentally determined void fractions. The void fractions were measured with a calibrated gamma densitometer. The results of this experiment are now being written up in an MS thesis by Mr. Chungliang Lin. Note that there is a reasonable agreement between the experiment and the theory.

Figure 7 shows the flow patterns in the fluid bed. The numbers are the instantaneous void fractions and the arrows indicate the gas and solid velocity components. We see that solids are entrained into the jet base and are carried up by the jet. We also see gas entrainment. There is a large-scale circulation which is caused by the average density differences in the bed. An approximate solution to the differential

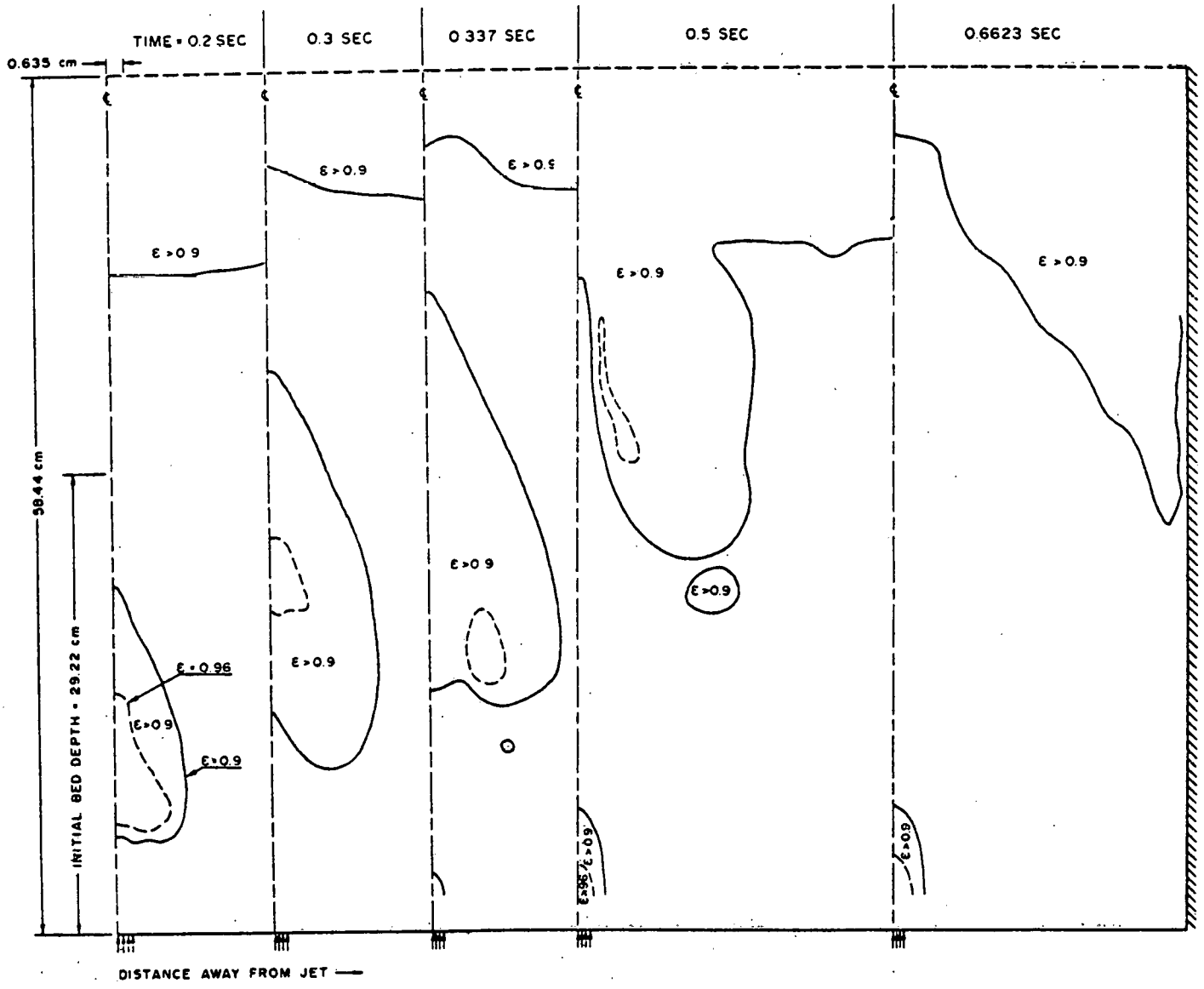

Fig. 4. Computed Growth and Collapse of a Void (Bubble) in a Fluidized Bed with a Jet. The minimum fluidization velocity is 0.416 m/sec. Jet was turned on at zero time with a velocity of 6.14 m/sec.

COMPUTED POROSITY PROFILES IN THE TWO-DIMENSIONAL FLUIDIZED BED WITH JET

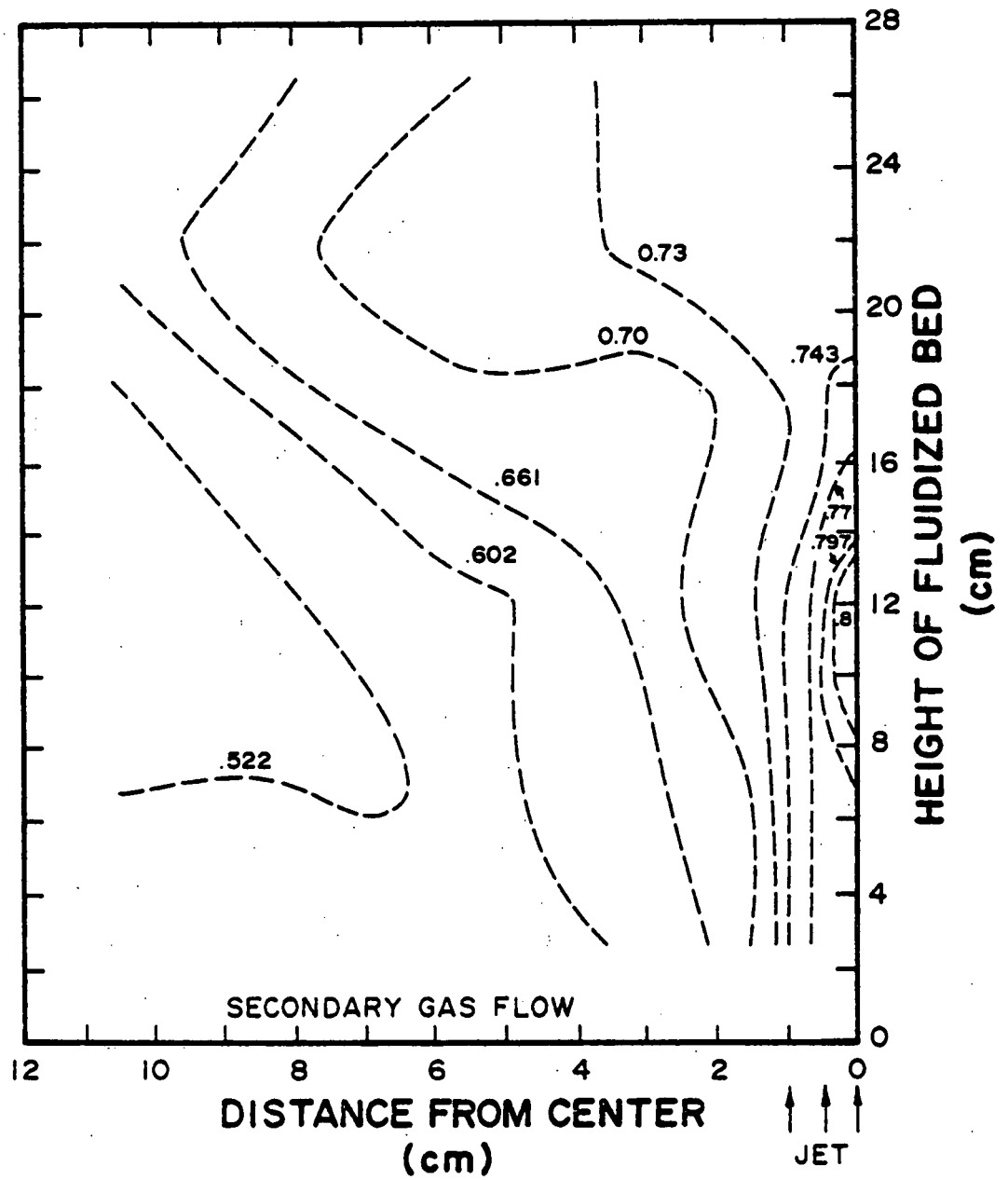

Fig. 5. Time averaged porosities

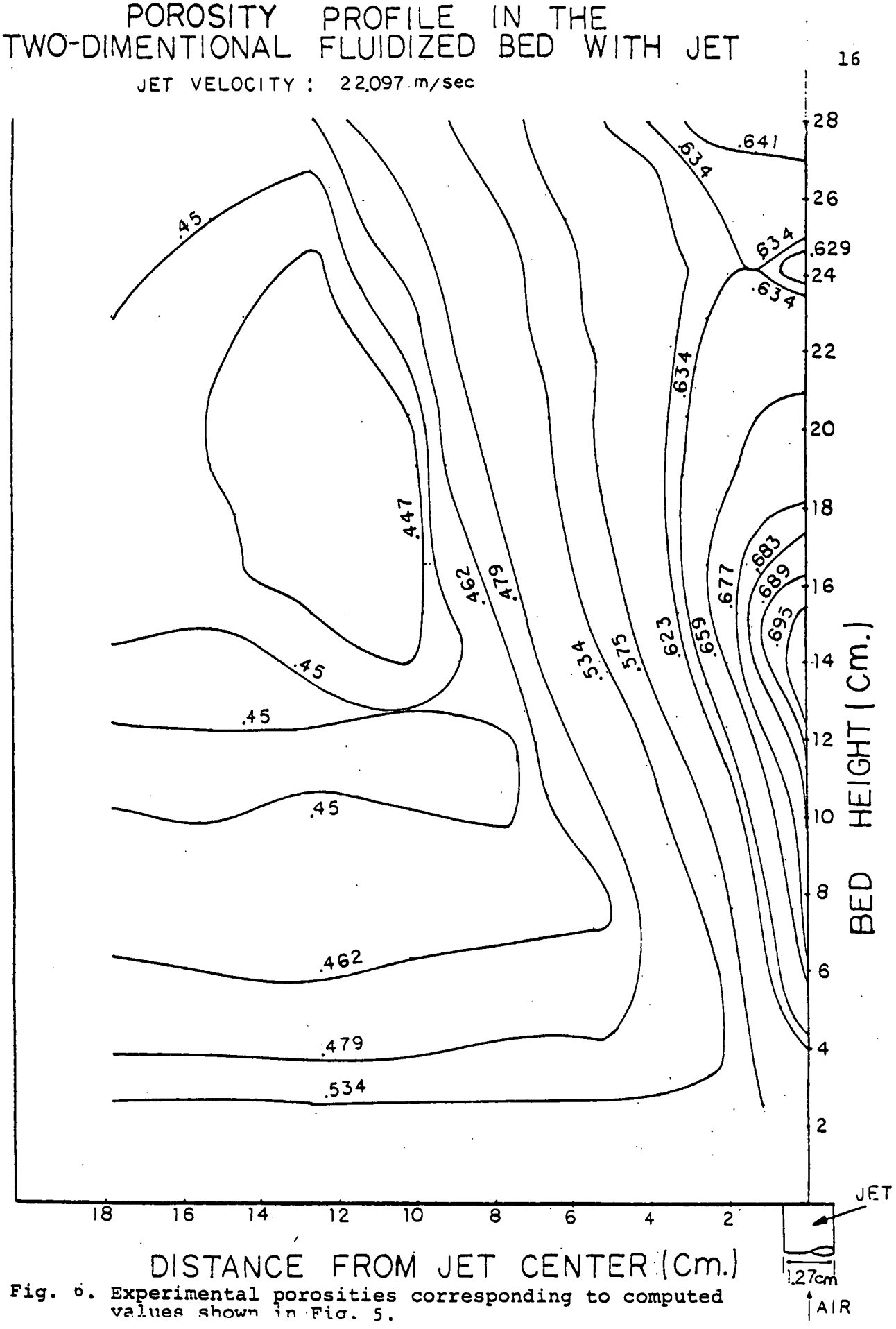

Fig. 6. Experimental porosities corresponding to computed values shown in Fig. 5.

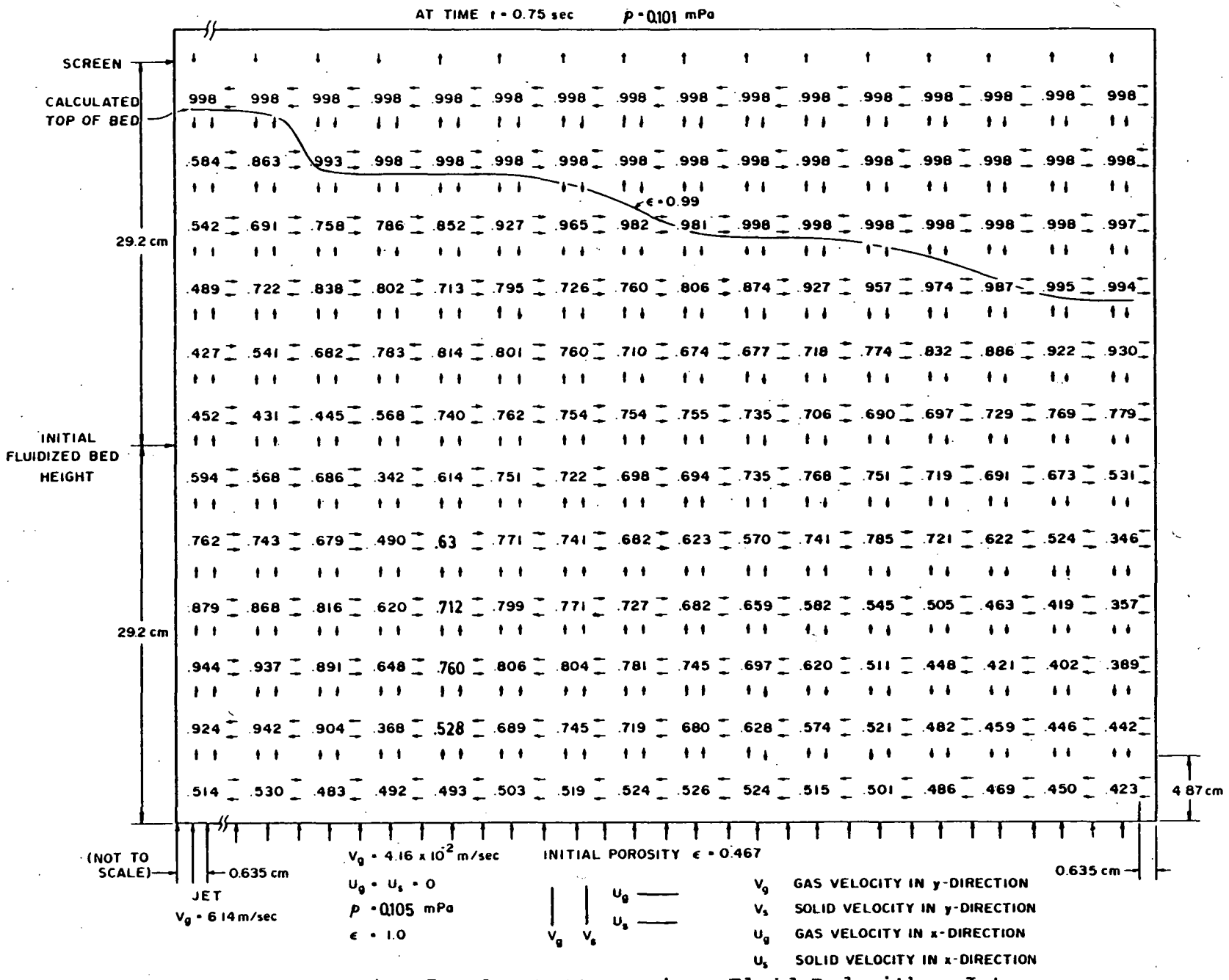

Fig. 7. Flow Patterns in a Fluid Bed with a Jet.

equation obtained by dividing the bed into a jet and downcomer regions showed that

$$\text{Solids circulation} = \sqrt{\varepsilon_{s_j}\, gx(\varepsilon_{sd} - \varepsilon_{s_j})}$$

where ε_{s_j} is the average void fraction in the jet and ε_{sd} is an average void fraction in the downcomer. In the above formula x is the bed height and g the gravity. This formula agrees within a factor of two with the more exact calculations. Better agreement is not expected due to the complex motion taking place in the two-dimensional bed.

Figure 8 shows instantaneous profiles of gas and solid velocities around the jet axis. The gas velocity is maximum at the jet entrance and decreases into the bed. Qualitatively, we see an agreement between this theory and the experiments of Yang and Keairns (1980) and others. Figure 8 also shows that the solids velocity reaches a maximum at a bed height of about 14.6 cm. Thus solids particles are picked up by the gas above the jet mouth, are accelerated up the bed, but then lose their momentum through the friction with the particles.

Figure 9 shows porosity and pressure fluctuations above the jet inlet from the time the jet was turned on. The porosity figure shows that there are 7 to 8 bubbles formed every second, since the porosity oscillates four times between the times 0.3 and 0.85 seconds. This can be compared to a formula given by Kunii and Levenspiel (1962)

$$n = 54.8/v^{1/5}$$

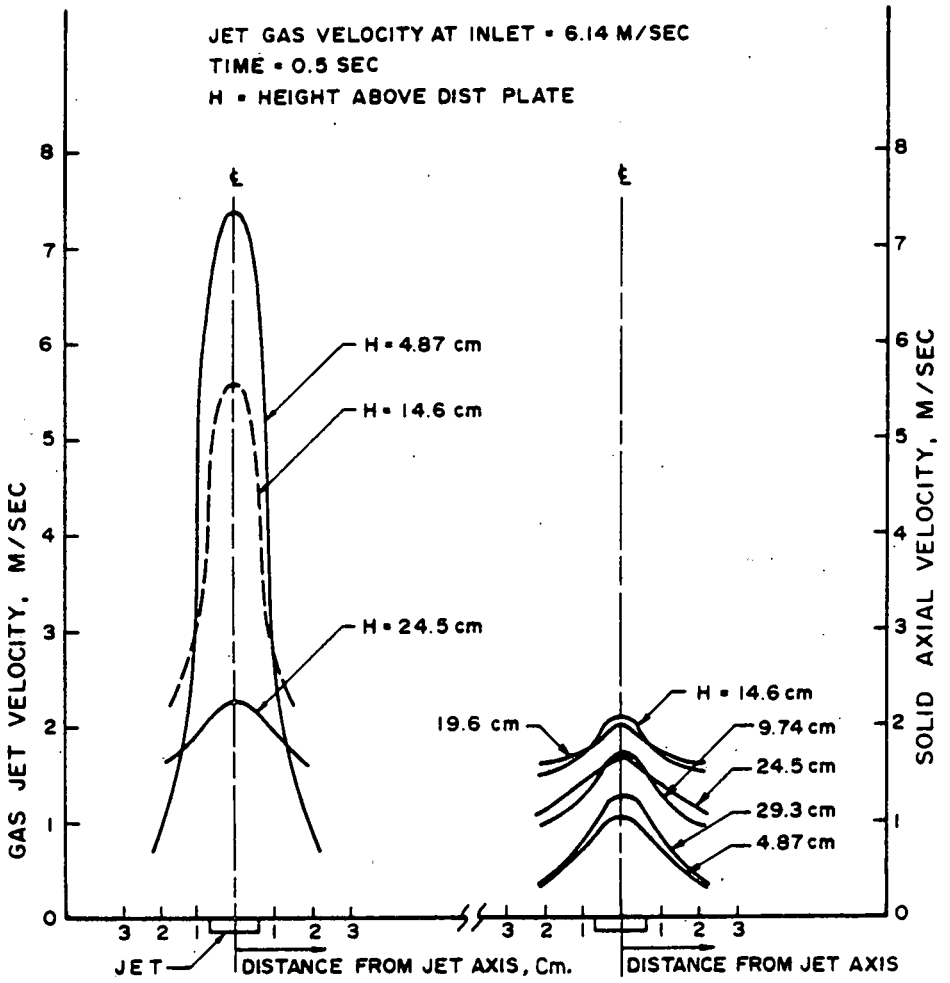

Fig. 8. Computed Instantaneous Gas and Solids Velocities of a Jet in a Fluidized Bed

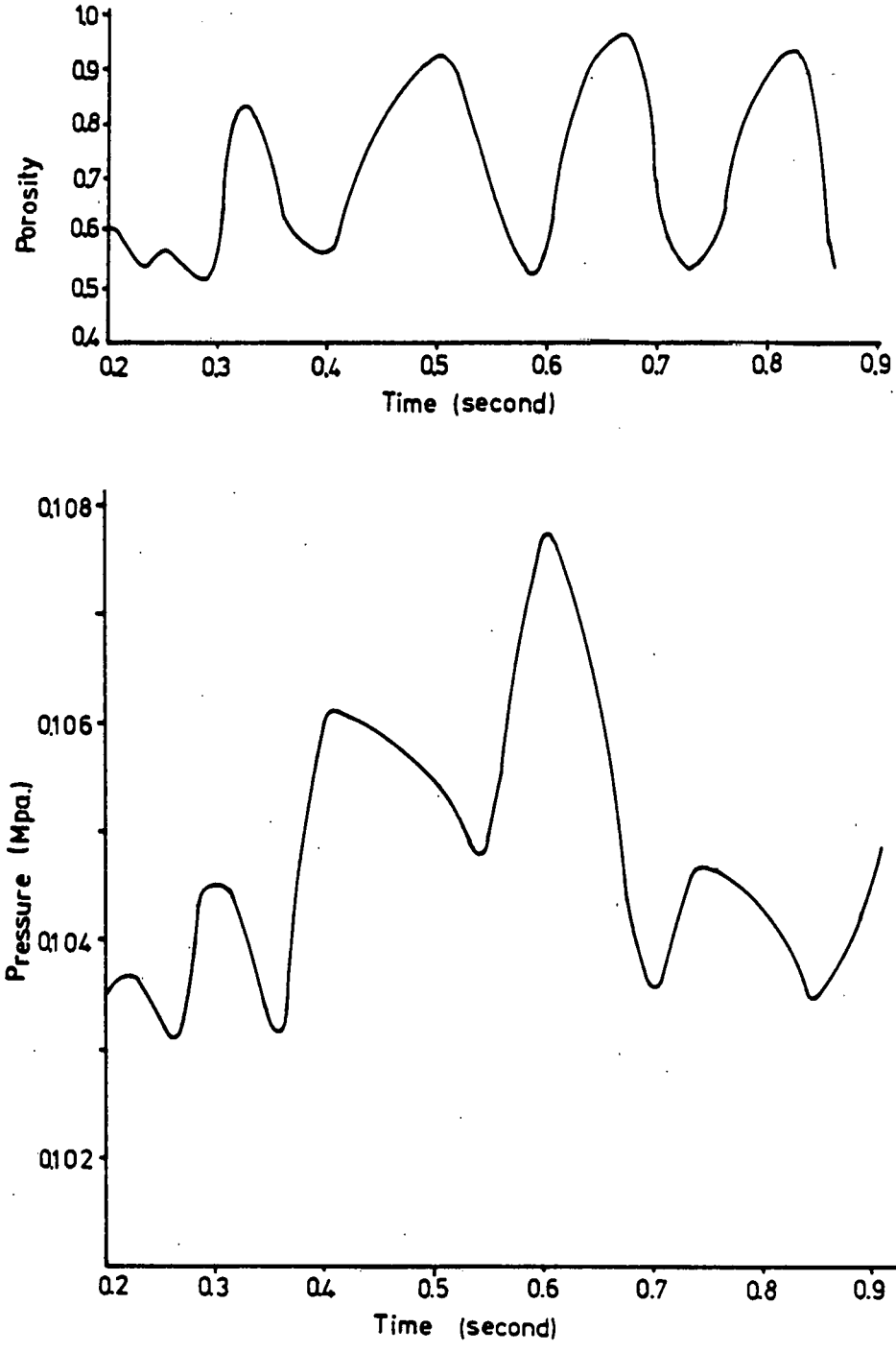

Fig. 9. Porosity and Pressure Oscillations at the Jet Inlet in a Fluidized Bed.

where n is the number of bubbles per second and v is the volumetric gas flow through a nozzle. For a jet velocity of 6.14 m/sec, the formula predicts 11 bubbles per second which is in reasonable agreement with the calculation in view of the differences of the physics. For a better comparison of the theory and experiment, density and pressure fluctuations must be measured with the two-dimensional bed in our laboratory.

SOLIDS CIRCULATION AROUND A JET

The calculation of solids circulation around a jet is complicated by the oscillatory nature of the jet in a fluidized bed due to bubble formation near the jet inlet and its motion through the bed. The calculation of solids flux involves the product of solids volume fraction and the solids velocity. Figure 10 shows the void fraction, that is one minus the solids volume fraction, along the jet for various times after jet start-up. At t = 0.0128 seconds, a bubble begins to form near the jet entrance. The bulk of the bed is still at minimum fluidization. There was still little bed expansion, since beyond 30 cm the bed is free of solids. At t = 0.2 seconds we see a bubble going through the bed. For the sake of the following discussion we define a bubble as a region of void greater than 0.9. Then we see that at a position of 4.4 cm the size of the bubble is 15 cm, that is we essentially have a slug of gas moving up. At 0.6 seconds, there is a bubble of width 5.6 cm at a distance of 22 cm from the inlet. Near the inlet a new bubble of width about 0.7 cm has formed. At 0.7 seconds, this new bubble has grown to a width of 8.3 cm. At 0.9 seconds it moved to a height of 13.2 cm and has decreased to a width of 5 cm.

Figure 11 shows the superficial velocity of the solid, that is the product of the solids volume fraction and the solids velocity at two time intervals along the length of the

VOID FRACTION ABOVE THE JET ENTRANCE ALONG THE JET AT DIFFERENT TIME-INTERVALS

t = Time [secs.]

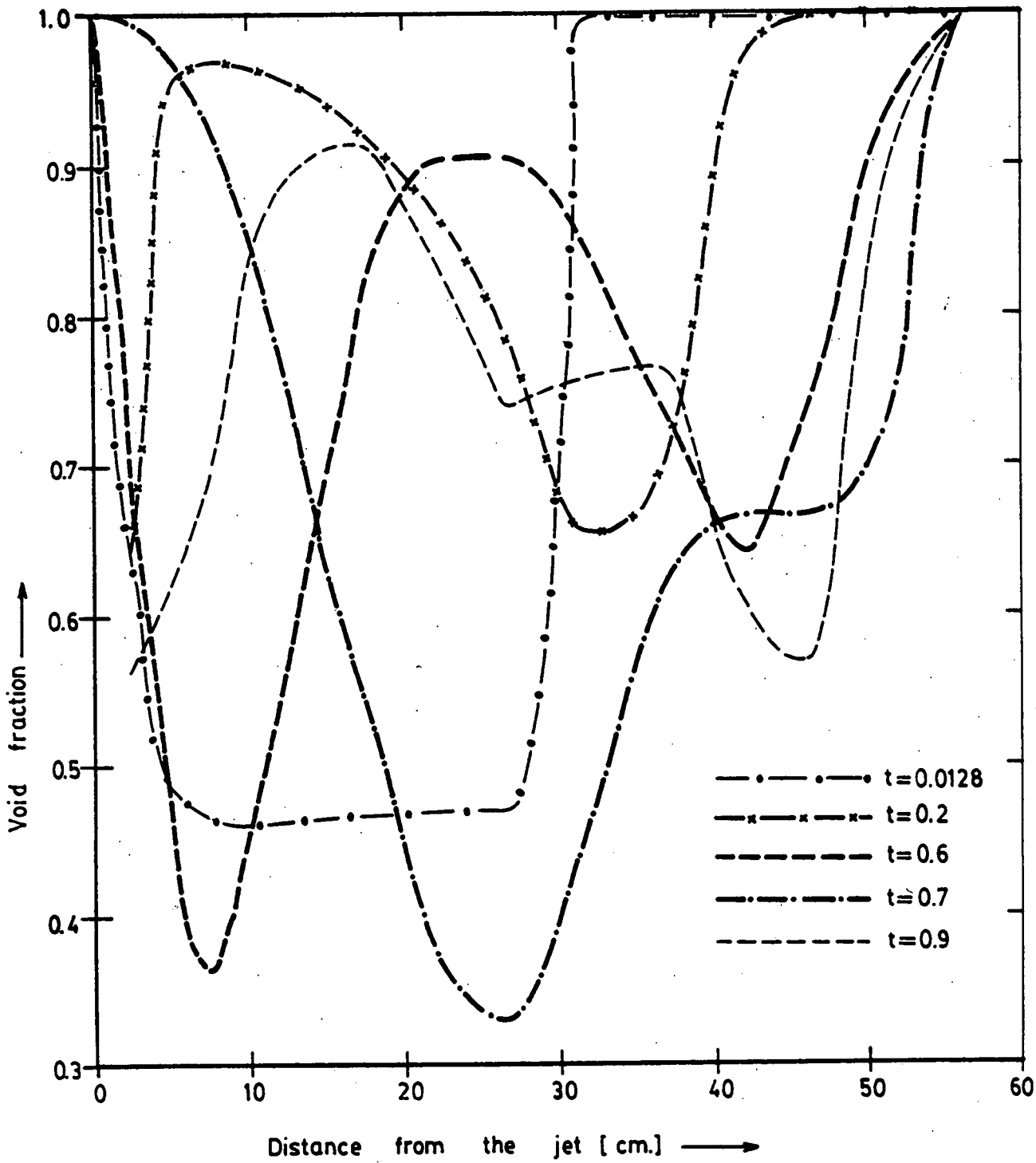

Figure 10.

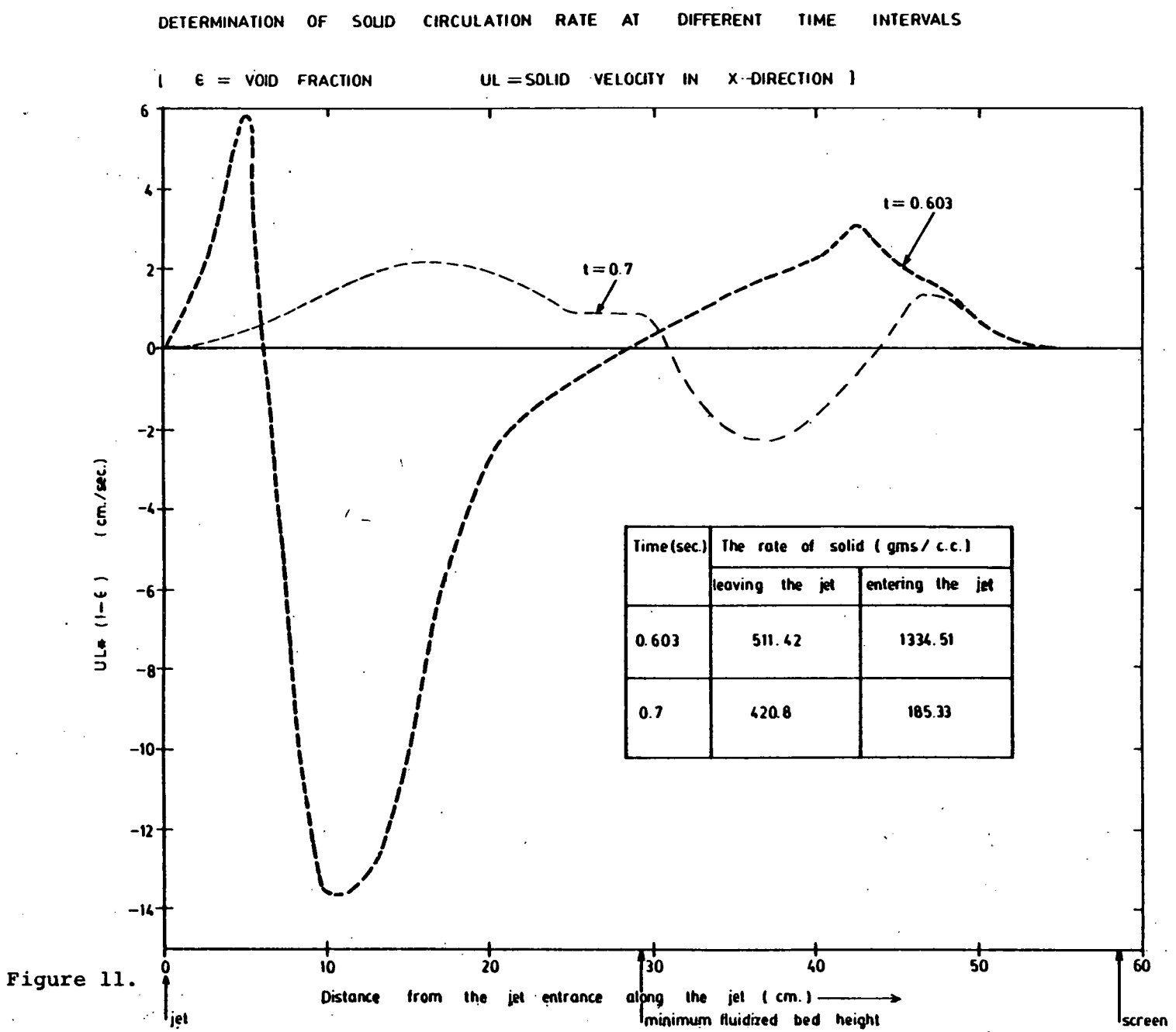

Time (sec.)	The rate of solid (gms / c.c.)	
	leaving the jet	entering the jet
0.603	511.42	1334.51
0.7	420.8	185.33

Figure 11.

jet. The negative velocity indicates the entrainment of the solid into the jet, while the positive velocity shows the solid leaving the jet. We clearly see the oscillatory nature of the process. The table in the figure shows that at any instant of time there is no balance between the rate of solid leaving and entering the jet. A balance exists only over a complete period of time. Hence at any time the rate of solid entering or leaving the jet can be expressed as

$$W_s = a\rho_s \int_{L_1}^{L_2} \epsilon_s U_s dy$$

where, a = thickness of the bed

ρ_s = solid density

ϵ_s = solid fraction

U_s = solid velocity in x-direction across the jet.

y = distance from the jet entrance along the height

L_1 to L_2 = length through which solid enters or leaves the jet.

As is clear from Figure 11, the lengths through which the solid is leaving or entering the jet varies with time.

The above expression can be used to determine the rate of solid leaving or entering the jet at any instant. As shown in Figure 11, the solid rates are calculated at t = .603 and .7 secs.

In the same manner the time averaged values of solids rates can be calculated for a particular time range. We chose the range such that it varies from t_1 to .9705 sec. By

assigning different values to t_1, different time averaged solid rates can be calculated.

Thus for various t_1, $\Delta Ws = Ws_{ent.} - Ws_{leav.}$

A plot of ΔWs with t_1 shows that at $t_1 = 0.2$, $\Delta Ws \simeq 0$ and again at $t_1 = .54$ and $.66$ secs. $\Delta Ws = 0$.

This suggests a periodic oscillation of ΔWs with t_1 of period = .66 - .2 = .46 secs.

Averaging the values of Ws entering or Ws leaving between the time interval 0.2-0.66 the average solid circulation rate can be calculated, which is equal to 275 gms/sec. We assume here that the steady state is attained at t = 0.2 secs. and the period of oscillation is 0.46 sec.

The computer program was also run on the Cray-1 machine for two other velocities,in addition to the previous jet velocity of 6.14 m/sec. The additional jet velocities were 4.8 m/sec and 2.58m/sec. These lower velocities were chosen to correspond to experimentally determined void fractions in a two dimensional fluid bed. The calculated solids circulation rates are shown in Figure 12. As expected, the solids circulation rate increases with velocity. Quantitative comparisons to experiments are not available. The case of solids circulation with a draft tube is discussed in another section. We believe that in view of the complex nature of the phenomenon of solids circulation, as discussed above, it is the individual solids and gas velocities and the void fractions that are needed in the design of gasifiers. Values of solids circulations are probably of only limited utility.

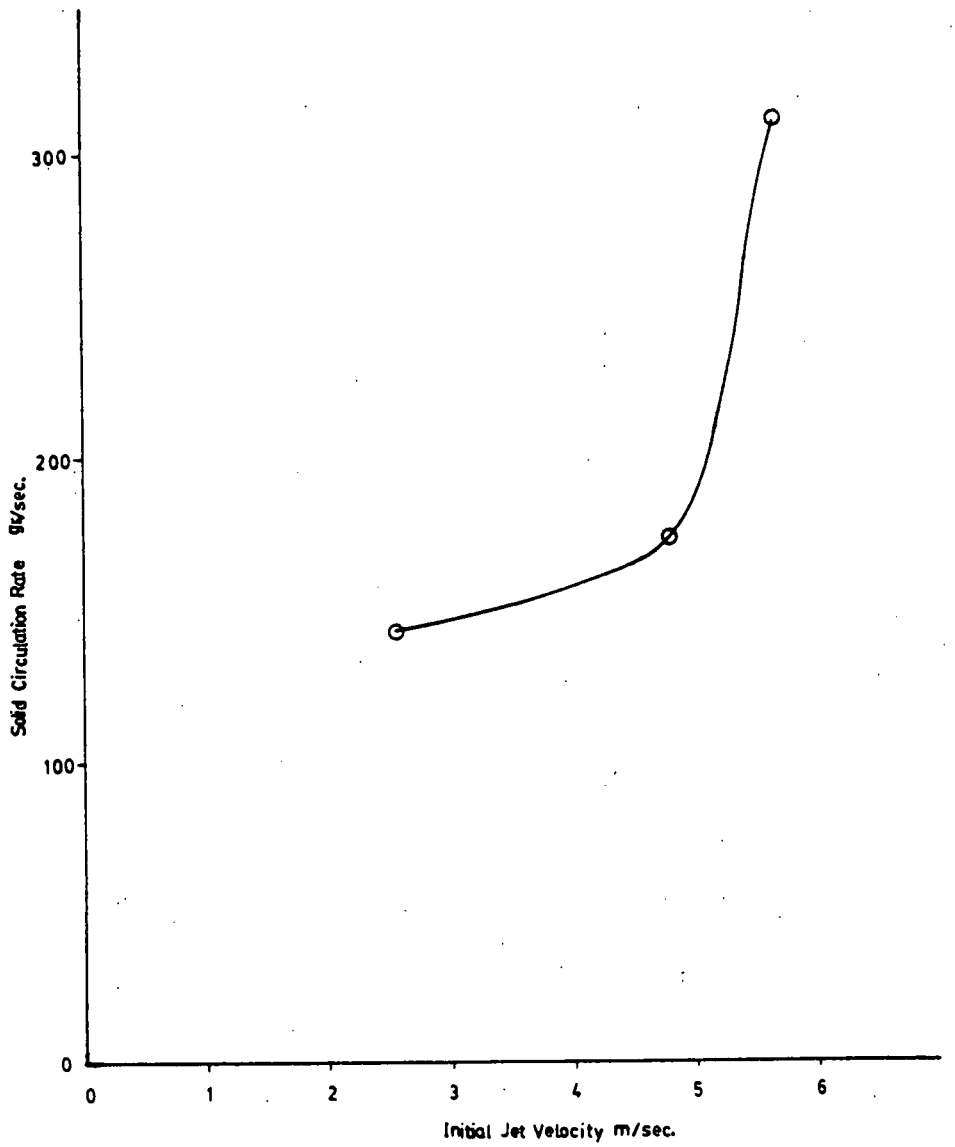

Figure 12. Computed Solids Circulations Rates for Two Dimensional Fluidized Bed with a Jet.

AN ANALYTICAL SOLUTION FOR SOLIDS CIRCULATION

To understand the behavior of solids circulation it is useful to obtain a simplified analytical solution to the problem. To do this a number of drastic assumptions must be made in the multidimensional two phase flow equations.

The first assumption is a geometrical one. The fluid bed is divided into two regions: a jet region and a downcomer region. Cross circulation caused by lateral motion of solids particles is neglected. Furthermore, based on order of magnitude estimates it is possible to:

(1) Neglect gas momentum with respect to solids momentum due to the much larger density of the solids compared with that of the gas

(2) Neglect the momentum head in the downcomer region due to small solids velocities

(3) Neglect wall friction

With these assumptions the mixture momentum equations become:

Mixture momentum in the jet region in conservative form

$$\frac{d}{dx}\left(\rho_s \varepsilon_{sj} U_{sj}^2\right) = -\frac{dP_j}{dx} - g\rho_s \varepsilon_{sj} \qquad (1)$$

Mixture momentum in the downcomer

$$\frac{dP_d}{dx} = -g\rho_s \varepsilon_{sd} \qquad (2)$$

Away from the entrance of the downcomer and the jet region, where the solids are accelerated to be carried pneumatically in the jet region, the momentum equations can be

expressed in integrated form. With constant solids volume fraction in each region, we then have the balances

$$\rho_s \varepsilon_{sj} U_{sj}^2 + P_j + g\rho_s \varepsilon_{sj} x = 0 \qquad (3)$$

$$\Delta P_d + g\rho_s \varepsilon_{sd} x = 0 \qquad (4)$$

Equation (3) is somewhat similar to Yang and Keairn's (1974) equation (16) for the draft tube. In equation (3) the wall friction has been neglected. Also the kinetic head does not have a factor of 1/2 in equation (3). This is because the mixture momentum equation has been integrated in the conservative form given by Equation (1). Integrating it in the form $\rho_s \varepsilon_{sj} U_{sj} \frac{dU_{sj}}{dx}$ leads to the 1/2 in the Yang and Keairn's formula. However, this involves an additional assumption of constancy of ε_{sj} throughout the draft tube. Integration of the mixture momentum equation in the conservative form only assumes that the solid entered the region with a zero velocity. Thus in equation (3) only the value of ε_{sj} in the gravity term has been assumed to be a constant. This constant may further be interpreted as an average value over the distance x.

Equation (4) states that the pressure drop in the downcomer region is all due to the weight of the solids, as is well known to be approximately true near minimum fluidization. Furthermore, the boundary conditions suggest that

$$\Delta P_j = \Delta P_d \qquad (5)$$

Elimination of the pressure drop in equation (3) gives

$$\rho_s \varepsilon_{sj} U_{sj}^2 = g\rho_s \times (\varepsilon_{sd} - \varepsilon_{sj}) \quad (6)$$

From continuity equation for the solid we knew that

$$\rho_s \varepsilon_s U_s = \text{constant} = W_s \quad (7)$$

where W_s is the recirculation rate of solids per unit area. Then multiplication of equation (6) by $\rho_s \varepsilon_{sj}$ and solution for W_s gives the desired formula.

$$\text{Solids circulation} = W_s = \rho_s \sqrt{\varepsilon_{sj} gx(\varepsilon_{sd}-\varepsilon_{sj})} \quad (8)$$

The above formula for solids circulation flux, W_s, states that circulation is caused by the differences in densities or solids volume fractions, $\varepsilon_{sd}-\varepsilon_{sj}$, between the two regions. Qualitatively, this has been known to be the cause of circulation in fluidized beds for many years. Davidson and Harrison's group has taken advantage of this cause to suggest various designs involving blowing gases at different flow rates at various bed positions. The solids circulation formula (8) is also related to the orifice formula, Equation (39) of Yang and Keairns (1974) and to the empirical correlations, equations (2) and (3) of Yang Keairns. All the formulae involve a driving head due to a column of a solids mixture.

In the solids circulation formula the void fractions in the two regions can be estimated similarly to that discussed by Yand and Keairns (1974). ε_{sd} can be obtained from the pressure drop which can be related to the friction given by the Ergun type equations. ε_{sj} can be approximately obtained

from a drag or friction between the phases type expression used by Yang and Keairns. In the final analysis, of course, it is best to substitute measured values.

Approximate Solids Circulation Formula

Away from the entrance region, gradients of relative velocity vanish and we can simply balance gravity with drag between the phases. Then for constant slips,

$$\beta(U_g - U_s) = g \tag{9}$$

where the friction coefficient β is related to the standard drag coefficient, C_d by the formula

$$\beta = C_d \frac{(1-\varepsilon)\mu}{\varepsilon^2 d^2 \rho_s} \tag{10}$$

Then substituting $W_s = \varepsilon_{sj}\rho_s U_{sj}$ into equation (9) the volume fraction of solids in the jet region is given by

$$\varepsilon_{sj} = \frac{W_s}{\rho_s}\left(\frac{1}{U_{gj}-g/\beta}\right) \tag{11}$$

and the solids circulation rate is

$$W_s = \frac{\rho_s \varepsilon_{sd} gx(U_{gj}-g/\beta)}{gx + (U_{gj}-g/\beta)^2} \tag{12}$$

Although in equation (12) β is implicitely a function of W_s through equation (10) and dependence of β on C_d, as in Arastoopour and Gidaspow (1979), the formula shows the dependence of circulation on jet velocity, U_{gj}, bed height, x and particle diameter, d.

For small slip velocity or large bed height,

$$W_s = \rho_s \varepsilon_{sd} (U_{gj} - g/\beta) \tag{13}$$

Thus for constant β, the circulation rate increases linearly with jet velocity under these conditions. For the other extreme there is a decrease of circulation with jet velocity. For constant β, there is a maximum circulation rate at the velocity

$$U_{gj,\ optimum} = \frac{g}{\beta} + \sqrt{gx} \tag{14}$$

given by

$$W_{s,max} = \frac{\rho_s \varepsilon_{sd}}{2} \sqrt{gx} \tag{15}$$

TABLE I. Comparison of Yang and Keairn's (1974) Data to Gidaspow's Theory

Run No.	Observed Solid Flow Rate kg/sec	Calculated Solid Flow Rate kg/sec	Deviations From Exp. %	Calculated Solid Flow Rate Gidaspow's Theory	Deviations From Exp. %	Superficial Gas Velocity in draft tube m/sec
1-1-1	.64	.46	-28.2	.65	+ 1.5	12.9
1-1-2	.70	.42	-40.8	.79	+12.8	9.6
1-1-3	.43	1.09	+153.4	.84	+95.0	6.0
1-2-1	.66	.47	-29.5	.67	+ 1.5	12.6
1-2-2	.62	.55	-10.3	.76	+22.6	9.3
1-2-3	.51	.58	+13.73	.88	+72.6	4.0
2-1-1	.41	.93	+125.9	.61	+48.7	9.9
2-1-2	.55	.68	+23.1	.72	+30.9	9.3
2-1-3	.58	.47	-18.9	.77	+32.7	8.3
2-1-4	.47	.44	-6.38	.80	+70.2	6.2
3-1-1	.69	.54	-22.9	.71	+2.9	11.6
3-1-2	.63	.59	-5.8	.75	+19.0	9.8
3-1-3	.58	.59	+3.1	.82	+41.4	7.6
3-2-1	.64	.59	-8.5	.67	+4.7	12.4
3-2-2	.67	.58	-13.6	.71	+5.9	11.3
3-2-3	.64	.58	-10.6	.74	+14.9	10.0
3-2-4	.59	.54	-8.5	.77	+31.6	8.8

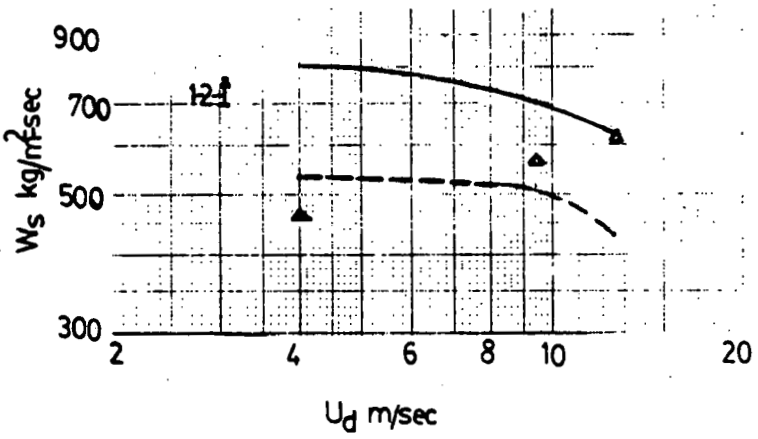

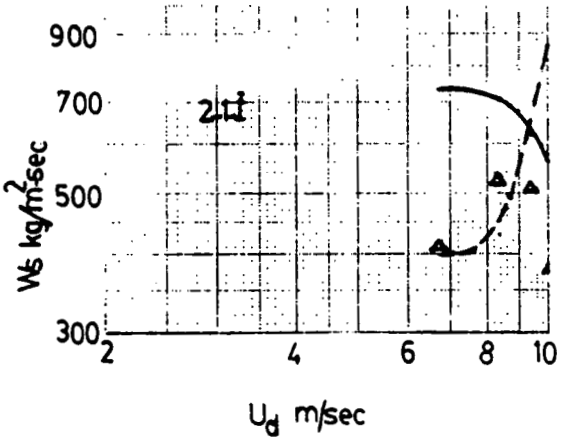

Kearns Data △

Kearns Theory - - - - - - -

Gidaspows Theory ———

U_d Superficial Gas Vel. in Draft Tube

W_s Solid Flow Rate Per Unit Area of Draft Tube

Figure 13. A Comparison of Solids Circulation Data with an Approximate Analytical Solution.

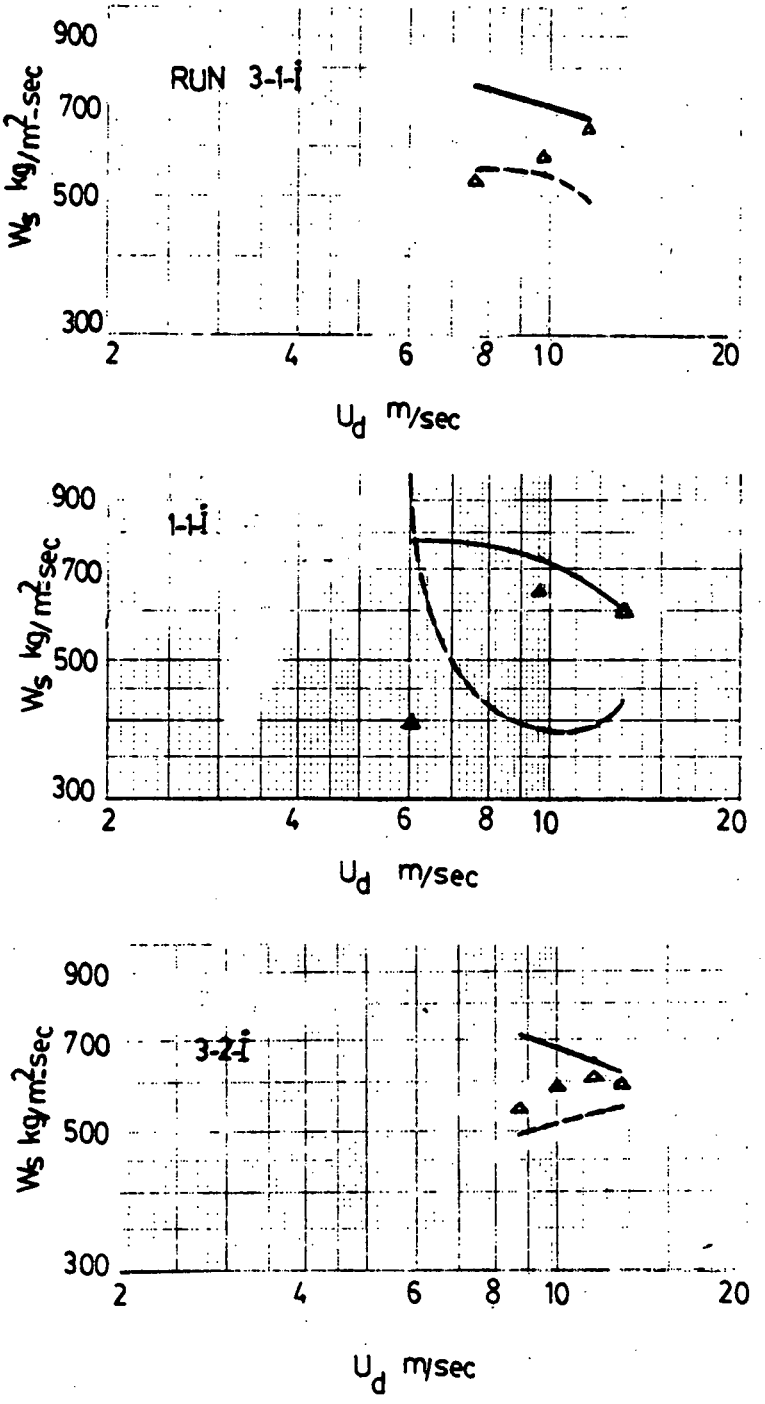

Figure 14. A Comparison of Solids Circulation Data with an Approximate Analytical Solution.

COMPARISON OF ANALYTICAL SOLUTION TO WESTINGHOUSE DATA

To judge the potential of the new approximate analytical formula for solids circulation, Equation (8) of Part 2 was compared with the Westinghouse cold model data reported by Yang and Keairns (1974). In the downcomer region, ϵ_{sd} was taken to be the minimum fluidization velocity equal to 0.467, calculated from the pressure drop using the Ergun equation. The void fraction in the jet region was found through Curran and Gorin's theory. These values give better results than those obtained with the use of Richardson and Zaki's relation. The circulation rates for the various jet nozzle positions, bed heights and air flow rates as reported by Yang and Keairns are shown in Table I and in the Figures 13 and 14.

It is clear that the approximate analytical formula roughly predicts the circulation rates. It is not much worse than Yang and Keairn's empirical formula. Agreement with the theory and data is better at high draft tube velocities.

APPARATUS FOR VOID FRACTION DISTRIBUTION

To give a complete comparison of data to theory, pressure, void fraction and the solid and gas velocities must be measured. Usually the void fraction has not been measured together with the other variables. For example, in the Westinghouse laboratories in Pittsburgh two and three dimensional beds have been constructed to simulate gasifier performance. The solid velocity is measured by a tracer (radio pill), the gas velocities by helium injection and the pressure with standard instruments. The void fraction is, however, not measured. Figure 15

shows the schematic of an apparatus which is being constructed to potentially measure all the necessary variables.

Time averaged void fractions have been obtained with a calibrated gamma ray densitometer. Figure 6 shows our preliminary data. Note that there is qualitative agreement between the data and the theory. The theory and the data both show a maximum void 10 to 12 cm above the jet inlet. The computed void fractions are about 15% higher. Data of the type shown in Figures 5 and 6 permits a rational calculation of jet penetrations. While there are various ways to define jet penetrations, note that Figure 8 shows that at a height of 14.6 cm, there is a maximum in the solids velocity. Keeping in mind that the velocities shown are instantaneous values, while the void fractions are time averaged, there is a close coincidence between the time the particles begin to slow down and between the area of maximum void.

Presentation of final experimental data and a comparison to theory and to literature correlations, such as those by Merry (1975) will appear in an MS thesis by Mr. Lin and in an annual report to the Gas Research Institute who have sponsored the final stages of this work.

SUMMARY OF AN ENTRAINED-FLOW GASIFIER MODELING (ENTRAINED-FLOW COAL HYDROPYROLYSIS REACTOR)

A mathematical model has been developed to describe physical and chemical processes occurring in an entrained-flow coal hydropyrolysis reactor. The model is one dimensional and incorporates a detailed multistep reaction kinetic developed

by Johnson for hydropyrolysis supplemented by Suuberg's pyrolysis model for rapid reactions, reactions of hydropyrolysis products in the gas phase, hydrodynamics of the gas-solid system, swelling/shrinking of the coal particles, and the heat transfer between the coal-char particles, gases and reactor walls. The system is described by fifty-three simultaneous non-linear first order ordinary differential equations. The solutions consist of time histories of quantities such as particle and gas temperatures, their compositions, velocities, and densities. This system of equations is very stiff primarily due to the high temperature dependence of various hydropyrolysis reaction rates. (A reviewer of this project had anticipated this phenomenon)

The reactor model has been used successfully in simulating Cities Service Research and Development Company's bench scale entrained-downflow hydropyrolysis tubular reactors (helically-entrained, vertically-entrained and free-fall) using Montana Rosebud subbituminous coal, Western Kentucky No. 9/14 bituminous coal, and North Dakota lignite as reactor feeds. The operating conditions of these simulated hydropyrolysis experimental runs ranged from 1403°-1697°F reactor temperature, 500-1600 psia reactor pressure, 0.18-1.3 H_2/coal wt. ratio and 0.3-24.7 sec. vapor residence times. Figures 16 and 17 show some typical results.

A detailed parametric study has also been performed using this model to identify important reactor parameters for the design of entrained-flow hydropyrolysis reactors. Three types

of coals, namely, Carco Texas lignite, Montan lignite, and Illinois No. 6 bituminous coals were studied for adiabatic reactor operation. In such adiabatic reactors, the necessary heat is mainly provided by the sensible heat of the preheated feed gas. The particle heating rate in such systems is very high and thus the particles and the gas approach their equilibrium mix temperature very rapidly. The effect of coal loading and inlet gas-solids mix temperature on the reactor performance were studied. For lower ranked (measured as the oxygen to carbon ratio in the coal) lignites, the reactor temperature drops rapidly near the entrance of the reactor due to strong endotherms evolving oxygenated gaseous species and thus much higher inlet mix temperatures are needed in such systems to achieve conditions adequate for the slower exothermic methane formation reactions to occur. For the higher ranked bituminous coal, no such significant temperature drop occurs even at moderate inlet mix temperature and the reactor temperature rises due to the exothermic reactions. Increasing the coal loading can increase or decrease the reactor temperature depending on the other operating conditions. The model allows a proper selection of inlet gas-solids mix temperature and H_2 to coal ratio for such reactor designs to avoid undesirable cold spots or hot spots in the reactors.

The rapid generation of volatile material decreases the heat transfer coefficient between the gas and the particle significantly, but only momentarily, and does not appear to affect the overall reactor performance. Also, the particle

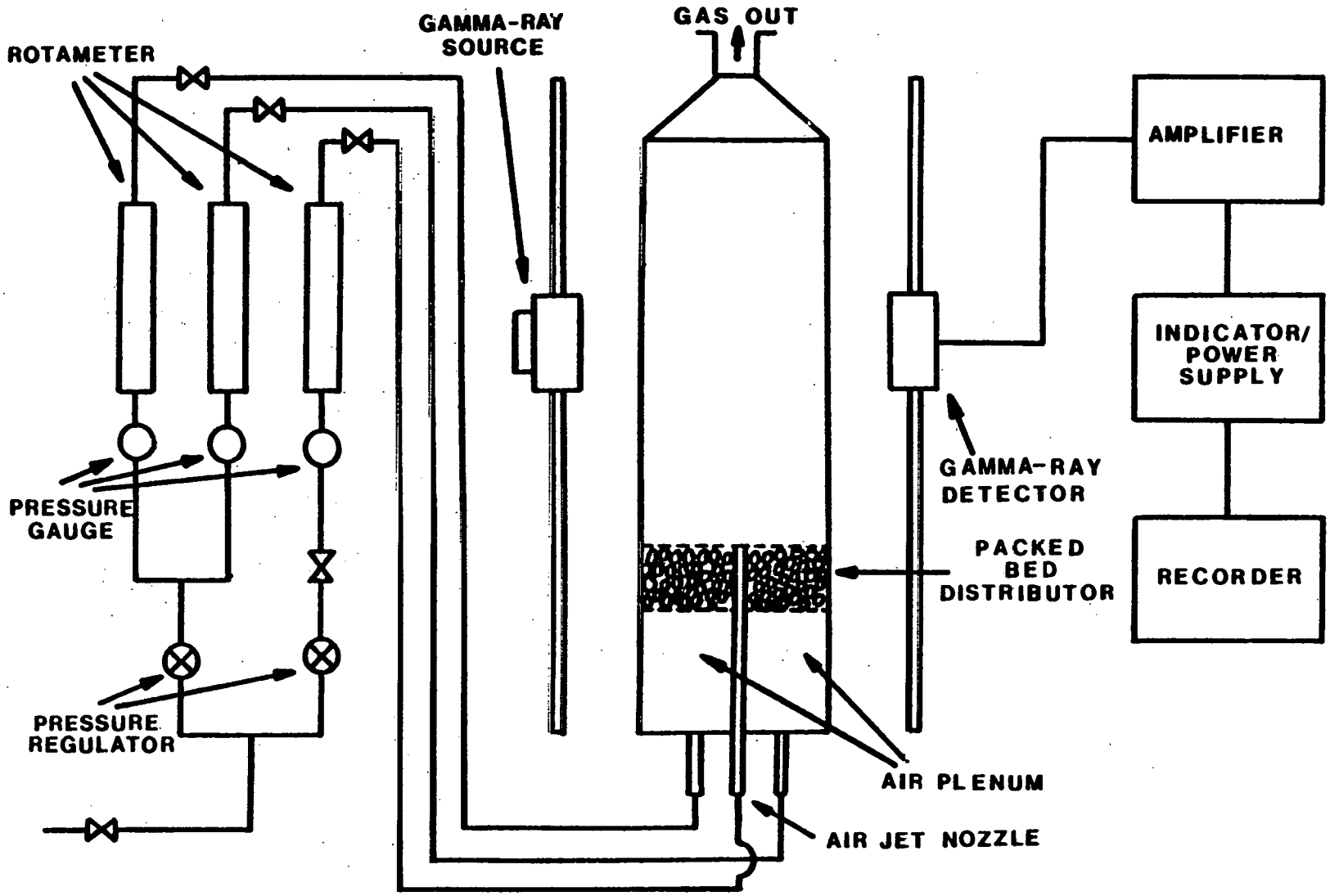

Fig. 15. Apparatus for Measuring Porosity in a Fluidized Bed.

swelling/shrinking (10-30%) does not significantly affect reactor performance. Particles, typical of such systems (< 200 μm), approach their equilibrium temperature very rapidly. Furthermore, as expected, higher inlet hydrogen pressure results in higher methane production.

One dimensional modeling with reaction kinetics and heat transfer is now complete and was presented in a Ph.D. thesis by A. Goyal, IIT, Chemical Engineering Department, May 1, 1980.

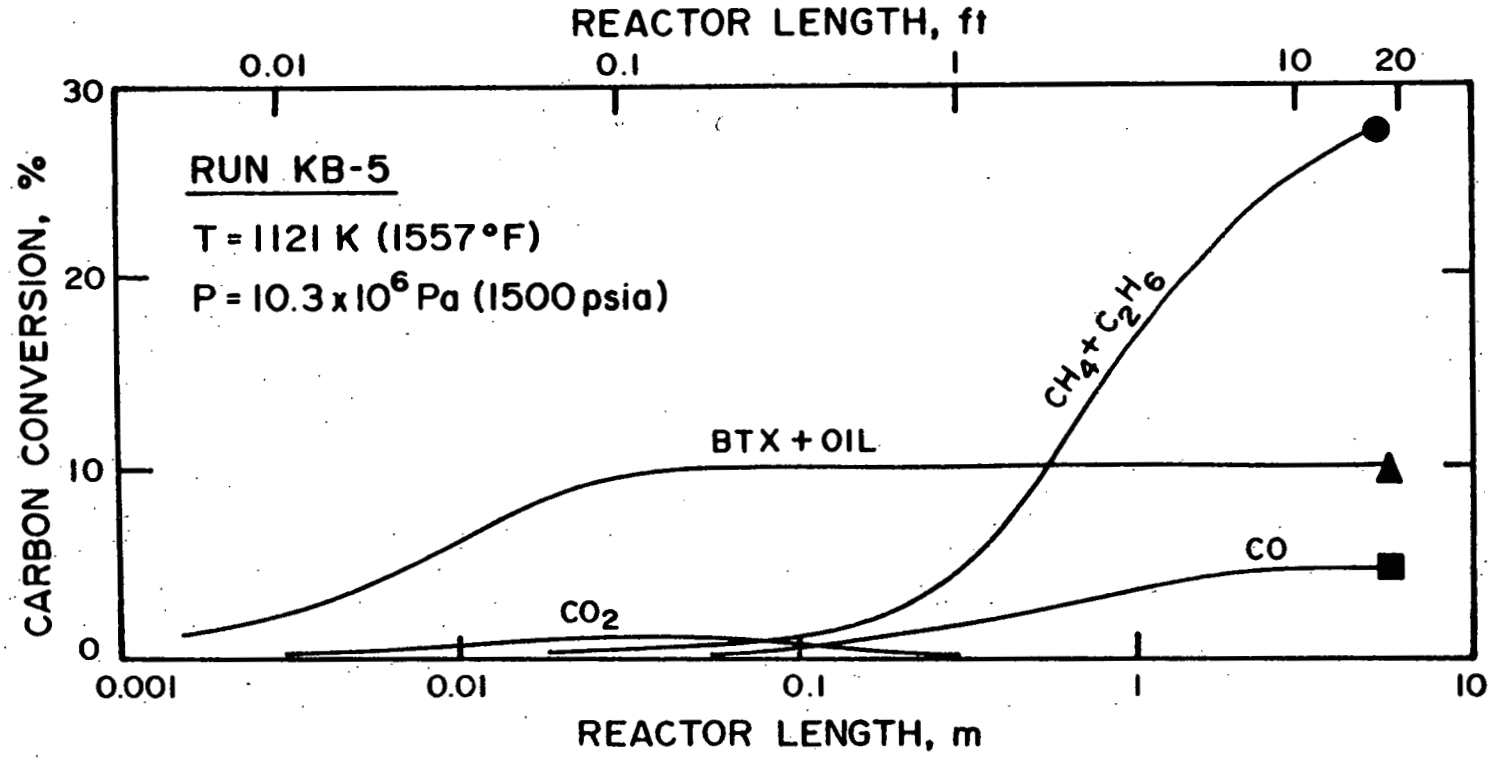

Figure 16. Distribution of Total Carbon Conversion to Different Species along Reactor Length — Run KB-5

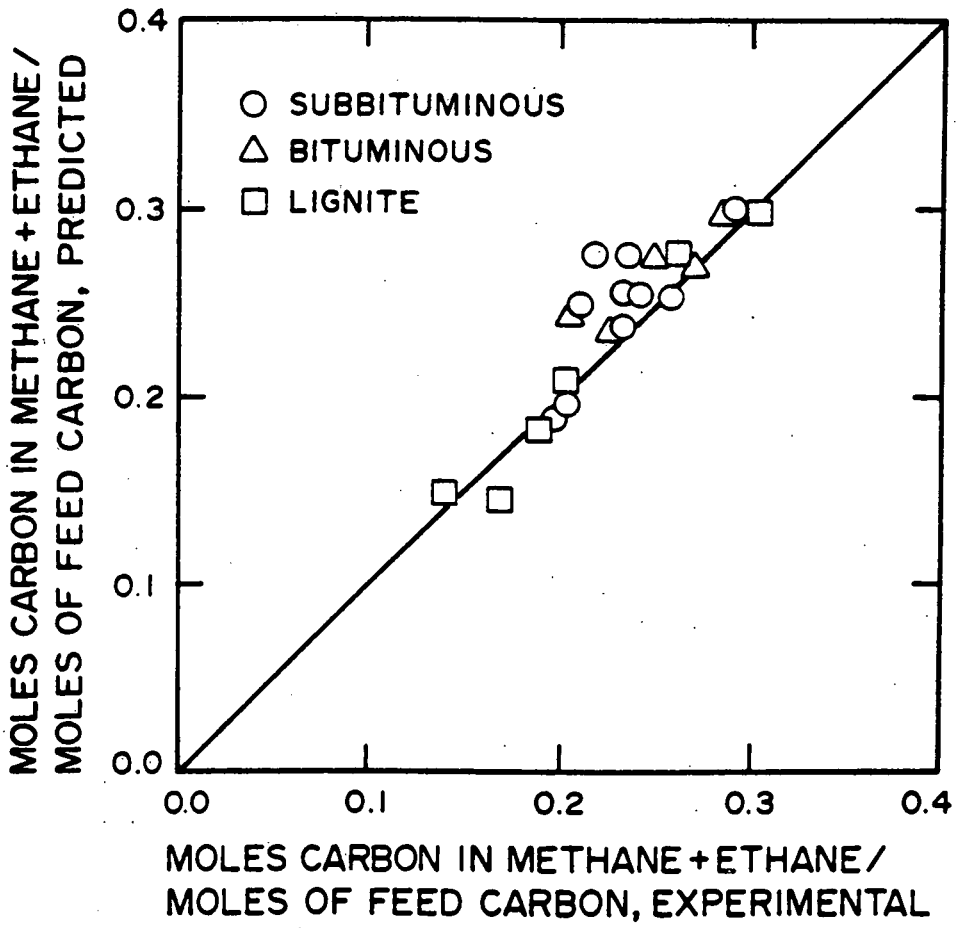

Figure 17. Comparison of Experimental and Predicted Methane + Ethane Yields - Cities Service Data

NOMENCLATURE

C_{D_s}	Drag coefficient	
dp, d	Diameter of solid particles	m
fwx, fwy	Wall, friction factors in x&y directions,	$Kg/m^2\text{-}sec^2$
g	Gravitation acceleration	m/sec^2
P	Pressure	Pa
Re_s	Solids Reynolds number	
T	Temperature	°C
t	Time	second
U_{mf}	Minimum fluidization velocity	m/sec
U_g	Lateral gas velocity	m/sec
U_s	Lateral solid velocity	m/sec
V_g	Axial gas velocity	m/sec
V_s	Axial solid velocity	m/sec
x	Co-ordinate in lateral direction	m
y	Co-ordinate in axial direction	m

Greek Letters

β	Friction coefficient	sec^{-1}
ε	Gas volume fraction	
μ	Gas viscosity	Kg/(m.sec)
ρ	Gas density	Kg/m^3
ρ_s, ρ_p	Solid and particle densities	Kg/m^3

Subscripts

d	downcomer region
g	gas
j	jet region
s	solid

Subscripts continued

x	in x direction
y	in y direction

REFERENCES

Anderson, T. B. and R. Jackson, A Fluid Mechanical Description of Fluidized Beds, Ind. Eng. Chem. Fundam. 6, 527-34 (1967).

Arastoopour, H. and D. Gidaspow, "Vertical Countercurrent Solids Gas Flow", Chemical Engineering Science. 34, 1063-66 (1979).

Arastoopour, H. and D. Gidaspow, "Analysis of IGT Pneumatic Conveying Data and Fast Fluidization Using a Thermohydrodynamic Model," Powder Technology 22, 77-87 (1979).

Arastoopour, H. and D. Gidaspow, "Vertical Pneumatic Conveying Using Four Hydrodynamic Models," I&EC Fundamentals, 18, 123-130 (1979).

Arastoopour, H., D. Lin and D. Gidaspow, "Hydrodynamic Analysis of Pneumatic Transport of a Mixture of Two Particle Sizes in Multiphase Transport: Fundamentals, Reactor Safety, Applications" editor, T. N. Veziroglu, Hemisphere Publishing Corp. (1980).

Babu, S. P., S. A. Weil & L. Anich, "Modeling of Coal Gasification Fluidized-Bed Reactors for Scale-up and Commercial Design" Institute of Gas Technology Annual Report to the American Gas Association (May, 1976).

Blake, T. R., D. H. Brownell, Jr. and G. P. Schmeyer "A Numerical Simulation Model for Entrained Flow Coal Gasification I. The Hydrodynamic Model," Presented at the Alternate Energy Sources Conference, Miami, Fl. (1979). Also "Numerical Simulation of Coal Gasification Processes" 87th AIChE Meeting, Boston (1979).

Bowen, R. M., "Theory of Mixtures" in "Continuum Physics, ed. A. C. Eringen, Vol. III, 1-127 (1976).

Davidson, J. F. Symposium on Fluidization-Discussion, Trans. Instn. Chem. Engrs. 39, 230-2 (1961).

van Deemter, J. J., Report on "Instabilities" Proceedings of the International Symposium on Fluidization in Eindhoven ed. A. A. H. Drinkenburg, Netherlands University Press, pp 91-98 (1967/68).

Drew, D. A., "Interfacial Momentum Transfer Models," 17th Annual Meeting of the Society of Engineering Science, Dec. 15-17 (1980).

Gary, S. K. and J. W. Pritchett, "Dynamics of Gas-Fluidized Beds", J. Appl. Physics 46, 4493-4500 (1975)°

Gidaspow, D., Round Table Discussion (RT-1-2), Modeling of Two-Phase Flow, 5th International Heat Transfer Conference, September 3, Tokyo, Japan, in Heat Transfer 1974, Vol. VII, pp. 163-68, 1974.

Gidaspow, D. and Solbrig, C. W., "Transient Two Phase Flow Models in Energy Production," State of the Art Paper presented at the AIChE 81st National Meeting, April 11-14 (1976); in revised form preprinted for NATO Advanced Study Institute on Two-Phase Flows and Heat Transfer, Istanbul, Turkey, August 16-27, 1976.

Gidaspow, D., "Hypertolic Compressible Two-Phase Flow Equations Based on S ationary Principles and the Fick's Law," in "Two-Phase Transport and Reactor Safety," Ed. by Veziroglu, T. N. and Kakac, S., 1, 283-298, Hemisphere Publishing Corp. (1978).

Gidaspow, D., and Y. W. Shin, "A Six-Equation Model for Transient, Two-Phase Flows by the Method of Characteristics" Argonne National Laboratory Report, in press (1980).

Jackson, R., The Mechanism of Fluidized Beds: Part I: The Stability of the State of Uniform Fluidization, and The Mechanism of Fluidized Beds: Part II: The Motion of Fully Developed Bubbles, Trans. Inst. Chem. Engrs. 41, 13-28 (1963).

Jackson, R., Chapter 3. Fluid Mechanical Theory, pp. 65-119 in Fluidization, edited by J. F. Davidson and D. Harrison, Academic Press, New York, 1971.

Kunii, D. and O. Levenspiel, Fluidization Engineering, Wiley and Sons, New York, 1969.

Lax, P. D., Differential Equations, Difference Equation and Matrix Theory," Comm. Pure and Appl. Math. 11, 175-94 (1958).

Lee, W. H., "A Pressure Iteration Scheme for Two-Phase Flow Modeling" in "Multiphase Transport" ed. T. N. Veziroglu, Hemisphere Publishing Corp. 1, 407-431 (1980).

Leung, L. S. "The Ups and Downs of Gas-Solid-Flow—A Review," in "Fluidization" ed. J. R. Grace and J. M. Matsen, Plenum Press, pp25-68, (1980).

Liu, Y., and D. Gidaspow, "Solids Mixing in Fluidized Beds—A Hydrodynamic Approach" Chemical Eng. Science, in press (1980).

Lyczkowski, R. W., Gidaspow, D., Solbrig, C. W. and Hughes, E. C. "Characteristics and STability Analyses of Transient One-Dimensional Two-Phase Flow Equations and Their Finite Difference Approximations," Nuclear Science and Engineering 66, 378-396, (1978).

Lyczkowski, R. W., D. Gidaspow and C. W. Solbrig "Multiphase Flow—Models for Nuclear, Fossil and Biomass Energy Production" to appear as a chapter in "Advances in Transport Processes" Wiley (1981).

Medlin, J., H.W. Wong and R. Jackson, "Fluid Mechanical Description of Fluidized Beds. Convective Instabilities in Bounded Beds," Ind. Eng. Chem. Fundam. 13, 147-59 (1974).

Merry, J. M. D., "Penetration of Vertical Jets into Fluidized Beds," AIChE Journal 21, 507-10 (1975).

Murray, J. D., "On the Mathematics of Fluidization. Part I. Fundamental Equations and Wave Propagation," J. Fluid Mech. 21, 465-93 (1965).

Pigford, R. L. and T. Baron, "Hydrodynamic Stability of Fluidized Beds" 4, 81-7 (1965).

Pritchett, J. W., H. B. Levine, T. R. Blake, S. K. Garg, "A Numerical Model of Gas Fluidized Beds," Presented at the AIChE 69th Annual Meeting, Chicago, Il., December 2, 1976. In AIChE Symposium Series Volume No. 176, 74, 134-148 (1978).

Richardson, J. F. and Zaki, W. N. "Sedimentation and Fluidization: Part I "Trans. Institute Chemical Engineers 32, 35-53 (1954).

Rivard, W. C. and J. R. Travis, "A Non-Equilibrium, Vapor Production Model for Critical Flow," Nuclear Science and Engineering 74, 40-8 (1980).

Rivard, W. C. and M. D. Torrey, "K-FIX: A Computer Program for Transient, Two Dimensional, Two Fluid Flow" Los Alamos, LA-NUREG-6623 (1977).

Rowe, P. N. Trans. Inst. Chem. Eng. 39, 175 (1961).

Rudinger, G. and A. Chang, Analysis of Nonsteady Two-Phase Flow, Physics of Fluids 7, 1747-54 (1964).

Ruckenstein, E. and Tzeculescu, M. "On the Hydrodynamics of the Fluidized Bed" in International Symposium on Fluidization, Eindhoven, 1967, ppl80-8, A.A.M. Drinkhenburg, editor, Netherlands University Press (1968).

Scharff, M. F., H. H. Klein, R.K.-C. Chan, D.E. Dietrich, S. R. Goldman and J. L. Sperling "Simulation of Cold Flow in Agglomerating Reactors" JAYCOR 510-80-006/2112 (July 1980).

Soo, S. L., Fluid Dynamics of Multiphase Systems, Blaisdell Publishing Co., Waltham, Massachusetts, 1967.

Soo, S. L. "Equations of Multiphase-Multidomain Mechanics" in "Multiphase Transport" T. N. Veziroglu, ed. Hemisphere Pub. Corp. 1, 291-305 (1980).

Wen, C. Y., "Optimization of Coal Gasification Processes" R&D Report No. 66 to the Office of Coal Research (1975).

Wen, C. Y., "Chemical Reaction in Fluidized Beds" in Proceedings of the NSF Workshop on Fluidization and Fluid-Particle Systems Research Needs and Priorities" pp317-387 (1979).

Wen, C. Y. and Y. H. Yu, Chem. Eng. Prog. Symp. Series No. 62, 62, 100 (1965).

Yang, W. and D. L. Keairns, "Momentum Dissipation of and Gas Entrainment into a Gas Solid Two-Phase Jet in a Fluidized Bed" in "Fluidization", ed. J. R. Grace & J. M. Matson, pp305-14 Plenum Press (1980).

W. C. Yang and D. L. Keairns, "Recirculating Fluidized Bed Reactor DAta Utilizing a Two Dimensional Cold Model" AIChE symposium Series No. 141, 70, 27-40 (1974).

ACKNOWLEDGEMENT

The latter phases of this work were partially supported by GRI Contract No.: 5014-363-0137, "Fluidization Using Non-Equilibrium Thermodynamics".

RE: "Multiphase Transport" ed. T.N. Veziroglu, Hemisphere Pub Corp. 4, 1853-71 (1980).

Hydrodynamic Analysis of Pneumatic Transport of a Mixture of Two Particle Sizes

H. ARASTOOPOUR and D. LIN
Department of Gas Engineering
Institute of Gas Technology
Chicago, Illinois 60616, USA

D. GIDASPOW
Department of Chemical Engineering
Illinois Institute of Technology
Chicago, Illinois 60616, USA

ABSTRACT

Three different models were used to predict pressure drop and segregation of particles flowing in a vertical pipe. One of the models was recently derived by the authors using an entropy production principle. The other models are the annular flow model and a simple Newton's law of motion for the particles.

All three of the models gave a reasonable prediction of pressure drop. The relative velocity model agreed well with experimental data. However, the predicted segregation of particles did not agree well with experimental data. This is due to the neglect of collisional frictional forces between type A and B particles which was neglected to avoid the use of fitted parameters.

INTRODUCTION

Pneumatic transport of a mixture of particle sizes is commonly used in conveyers and may soon be used in fluidized bed coal gasifiers. Two distinct particle sizes are taken advantage of in ash agglomerators to continuously remove ash from coal char. This paper is thus a first step toward an understanding of solids mixing phenomena in such gasifiers.

For uniform particle sizes, several previous investigators have used hydrodynamic equations. Examples are studied by Soo [2], Shook and Masliyah [8], Chandok and Pei [9], and Arastoopour and Gidaspow [10], [11]. There are four types of proposed unequal velocity models in the literature as classified by Gidaspow [3]. These models are a model with pressure drop in all phases (Case A), a model with pressure drop in the gas phase only (Case B), a relative velocity model derived using non-equilibrium thermodynamics (Case C), and a model with partial pressure drop in all phases (Case D). The partial pressure drop model was not able to predict reasonable values for solid-gas transport of uniform particles [5]. Thus there remain three unequal velocity models applicable to solid gas transport.

For binary solid mixtures Nakamura and Capes [1] used a hydrodynamic approach with constant phase velocities and a collisional force correlation. In addition to the pressure drop and choking velocity, they also analyzed

the segregation of different size particles. Yang [12] developed a segregation model for particles, based on the continuity equations of solids, particle velocity, solid friction factor, and pressure drop due to solid friction. He did not consider the momentum equations for the solid phases.

In this study we use hydrodynamic equations and consider each particle size as a different phase. Therefore for the transport of a mixture of two sized particles, we have three phases. Phases 1 and 2 are solids of different sizes and phase 3 is the gas. The solids-gas flow system is formulated by four different hydrodynamic models. Cases (A) and (B) are derived similarly to the two phase flow situation. For Case (C), the relative velocity model, Arastoopour [5] formulated the three phase flow equations in a manner similar to that used in the two-phase flow entropy-derivation of Gidaspow [3], [4]. This paper presents a numerical solution to these models and a comparison with Nakamura's and Capes' experimental data.

Three Velocity Models

The binary solids-gas mixture system can be described by means of one-dimensional, isothermal steady-state mass and momentum balances. The one-dimensional approximation is probably better for vertical than for horizontal transport due to settling in horizontal flow near saltation velocity. The isothermal assumption is a good approximation for dispersed flow due to good heat transfer to the wall and low rates of heat generation by friction.

Particle wall friction and friction between particles of two different sizes have been neglected in this analysis in an attempt to model this system without curve fitted parameters. In a more complete model such interactions must be included. However, data for such friction factors were not available.

The three continuity equations for the gas, the solid A, the solid B and the mixture momentum equation are –

Continuity Equations

$$\text{Gas Phase:} \quad \frac{d}{dx}\left[\varepsilon \rho_g V_g\right] = 0 \tag{1}$$

$$\text{Solid A Phase:} \quad \frac{d}{dx}\left[\varepsilon_A \rho_A V_A\right] = 0 \tag{2}$$

$$\text{Solid B Phase:} \quad \frac{d}{dx}\left[\varepsilon_B \rho_B V_B\right] = 0 \tag{3}$$

Mixture Momentum Equation

$$\varepsilon_g \rho_g V_g \, dV_g/dx + \varepsilon_A \rho_A V_A \, dV_A/dx + \varepsilon_B \rho_B V_B \, dV_B/dx = -\frac{dP}{dx}$$

$$- [\varepsilon_g \rho_g + \varepsilon_A \rho_A + \varepsilon_B \rho_B] \, g + f_w \qquad (4)$$

Solid A and B particles are incompressible. The gas phase is assumed to be compressible. The ideal gas equation of state is assumed to hold for gas. We want to determine the gas velocity V_g, the solid velocities V_A and V_B, the system pressure, P, and the volume fractions, ε_g and ε_A. We have ($\varepsilon_B = 1 - \varepsilon_A - \varepsilon_g$). Therefore, two more equations are needed. These two equations are the phase momentum equations for solids A and B, which differ from model to model, used in the literature:

Case (A): Pressure Drop in All Solids and Gas Phases [Annular Flow] e.g., Nakamura and Capes [1]

$$\rho_A V_A \, dV_A/dx + dP/dx = f_A - \rho_A g \qquad (5)$$

$$\rho_B V_B \, dV_B/dx + dP/dx = f_B - \rho_B g \qquad (6)$$

Case (B): Pressure Drop in Gas Phase Only, e.g., Soo [2]

$$\rho_A V_A \, dV_A/dx = f_A - \rho_A g \qquad (7)$$

$$\rho_B V_B \, dV_B/dx = f_B - \rho_B g \qquad (8)$$

Equations (7) and (8) are simply a statement of Newton's second law of motion for particles A and B, respectively, disregarding added mass forces.

Case (C): Relative Velocity, Gidaspow, [3], [4]; Arastoopour, [5].

Gidaspow [3], [4] developed a new model for solid-gas two phase systems using the methods of nonequilibrium thermodynamics. Minimization of entropy production gave a relative velocity equation of the form of Newton's second law of motion, with the velocity, however, being a relative solid-gas velocity. Arastoopour [5] followed this approach and

derived corresponding equations for a three phase mixture. Neglecting the interaction between particles A and B, Arastoopour's solids-phase momentum equations are –

$$1/2\ d/dx\ (V_g - V_A)^2 = -f_A/\rho_A + g \tag{9}$$

$$1/2\ d/dx\ (V_g - V_B)^2 = -f_B/\rho_B + g \tag{10}$$

Note that these differ from Equations 7 and 8 only by the presence of relative velocity. In the above equations, f_w, f_A and f_B are wall friction and drag force per unit volume of particles A and B, respectively. The frictional force, f_w, between the gas and the wall, can be expressed by means of the usual Fanning's Equation,

$$f_w = \frac{f_g \rho_g V_g^2}{2D} \tag{11}$$

where f_g, the friction factor, is a function of gas Reynolds' number and relative roughness of the pipe. The pipe was assumed smooth in our calculation. Therefore, f_g is a function only of the gas Reynolds' number. For the lower Reynolds' number, the friction factor can be obtained from the empirical Blasius formula:

$$f_g = \frac{0.316}{R_{eg}^{1/4}} \qquad \text{for } R_{eg} < 100{,}000 \tag{12}$$

For higher gas Reynolds' numbers, the friction factor can be obtained from the following expression (Handbook of Natural Gas Eng. [6]):

$$\frac{1}{\sqrt{f_g}} = 2 \log (R_{eg} \sqrt{f_g})^{-0.8} \tag{13}$$

The drag force, f_A and f_B, exerted by gas on the solid particles A and B per unit volume of particles, can be written as follows:

$$f_A = 3\ C_{DA}/4\ \frac{\rho_g (V_g - V_A)}{d_A}\ |V_g - V_A|\ \varepsilon_g^{-2.65} \tag{14}$$

$$f_B = 3\, C_{DB}/4\, \frac{\rho_g (V_g - V_B)}{d_B}\, |V_g - V_B|\, \varepsilon_g^{-2.65} \qquad (15)$$

The above correlations for the drag force are valid for spherical particles, where d_A and d_B are the particle diameters of solids A, can B and C_{DA} and C_{DB} are the drag coefficients. The drag coefficient can be related to the Reynolds' number by means of the relations –

$$C_{DA} = 24/R_{eA}\,(1 + 0.15\, R_{eA}^{0.687}) \quad R_{eA} < 1000 \qquad (16)$$

$$C_{DA} = 0.44 \quad R_{eA} > 1000 \qquad (17)$$

$$C_{DB} = 24/R_{eB}\,(1 + 0.15\, R_{eB}^{0.687}) \quad R_{eB} < 1000 \qquad (18)$$

$$C_{DB} = 0.44 \quad R_{eB} > 1000 \qquad (19)$$

where,

$$R_{eA} = \varepsilon_g \rho_g d_A (V_g - V_A)/\mu_g \qquad (20)$$

$$R_{eB} = \varepsilon_g \rho_g d_B (V_g - V_B)/\mu_g \qquad (21)$$

The three continuity equations, a mixture momentum equation, plus two solid-phase momentum equations which are different for different cases are the three sets of six nonlinear, first order differential equations. These six ordinary differential equations describe the solids-gas flow system. The Runge-Kutta method was used to obtain the numerical values for the above three sets of nonlinear first order differential equations.

Parametric Study Using a Thermodynamic Model

The vertical pneumatic transport studied here is the same as that used by Nakamura and Capes (1976) in their theoretical and experimental study on vertical pneumatic conveying of binary particle mixtures. The diameter of the conveying pipe was 1.18×10^{-2} meter and its length was 9.144 meter. The experiments were made with air as the gas phase and spherical glass beads of two different sizes as the solid phases. One solid phase is the solid A of density 2.90×10^3 kg/m^3 and particle diameter of 1.08×10^{-3}m. The other is the solid B of density 2.86×10^3 kg/m^3 and particle diameter of 2.90×10^{-3} m. In the

Nakamura's and Capes' experiment, the superficial air velocity U_g, the solid flow rate W_s, and the solid volume fractions ratio in the feed X_A were measured.[9] The pressure drop and average segregation were measured in the test section of an established flow above the acceleration zone. The length of this test section was 5.16 meters.

To compare the Nakamura's and Capes' experimental data with the present numerical calculations, in addition to the above mentioned measured values, the gas and the solid volume fractions and the total pressure at the inlet or at some arbitrary point along the pipe are needed. Since Capes and Nakamura did not report these quantities, reasonable numbers were chosen. Figures 1 and 2 show typical solids and gas velocity profiles along the pipe using the relative velocity model at a solid mass flow rate of 20.35 kg/sq m-sec. The initial volume fraction of gas and solid A are 0.995 and 0.475×10^{-3}, respectively. In Figure 1 we see that both solids A and B have been accelerated by the gas. Figure 2 shows the effect of a lower superficial gas velocity. Here we see that the velocity of larger particles decreases. As expected, the velocity of smaller particles (A) is lower than that in Figure 1. In Figure 2, we also see a greater change in gas velocity than in Figure 1. This is due to a larger particle concentration caused by the lower gas velocity.

The effect of the initial gas velocity was calculated at the initial pressure and volumetric concentration of $P_1 = 1.723 \times 10^5$ N/sq-m and $\varepsilon_{g_1} = 0.995$ respectively. As physically expected, the lower initial gas velocity results in lower solid velocities through the conveying line. At a very low gas velocity, such as at $U_{g_1} = 10$ m/sec, the solid B velocity decreases, due to gravity force dominating over the drag force. This results in a significant segregation between solids A and B, as is shown in Figure 3. Following Nakamura and Capes, the segregation along the pipe can be expressed by the solid volume fraction ratio, x_A/X_A:

$$x_A/X_A = \left(\frac{\varepsilon_A}{\varepsilon_A + \varepsilon_B}\right) \Big/ \left(\frac{\varepsilon_{A_1}}{\varepsilon_{A_1} + \varepsilon_{B_1}}\right)$$

The detailed parametric study showing the effect of initial velocities, concentrations, pressure and segregation was done by Lin (1978).

Comparison of the Three Unequal Velocity Models

The calculated pressure drop, phase velocities and solid segregation were compared with one another using the different models for flow of air and spherical glass beads of two different sizes through a vertical pipe. The vertical pneumatic transport studied here is the same as that used by Nakamura and Capes [1]. The solid mass flow rate and the initial pressure are 20.35 kg/sq m-sec and 1.723×10^5 N/sq m respectively. The initial superficial gas velocity is $U_{g_1} = 15$ m/sec with an assumed inlet gas

volume fraction of $\varepsilon_{g_1} = .995$. Figure 4 shows the calculated dimensionless solid velocities using the different models. All three cases A, B, and C show that the solid velocities increase through the vertical line. Cases A and B, the pressure drop in three phases and in gas phase, predict the same values for solid velocities through the line due to the low volume fraction of the particles in the mixture. They also predict a higher exit solid velocity than the relative velocity model due to an absence of an interaction effect among the phases for Cases A and B. Case C predicts a gradual increase in solid velocities, while Cases A and B show a sudden increase in solid velocities at the entrance.

Figure 5 shows the pressure drop versus the superficial gas velocity at a constant solid mass flow rate calculated using the three models. These three models show the experimentally observed choking behavior and a minimum in pressure drop. The minimum pressure drop is shown at the superficial gas velocity of 17 m/sec. At the gas velocities higher than 17 m/sec, the gas-solids mixture becomes dilute. The change in frictional force and velocity head predominate over the static head, and therefore the pressure drop increases with velocity similar to single phase flow. At very low gas flow rates, the friction and the velocity heads are small compared with the gravity term. The pressure drop is almost equal to the weight of the solids. This phenomena is qualitatively well understood. However, quantitative predictions are necessary for design. In approaching the much lower gas flow rate, the bulk density of gas-solids mixture becomes too great to support the solids, and the solids collapse into a slugging state.

Figure 6 shows the effect of the superficial gas velocity on the segregation of solids calculated using the three unequal velocity models. Case C, the relative velocity model shows a lower segregation due to greater interactional forces between the phases present in this model.

Comparison with Experiment

In order to compare our calculated results with Nakamura's and Capes' experiment, the same initial conditions and the same solid particles, gas and vertical tube were used. From the experiment, the solid mass flow rate W_s, the superficial gas velocity U_g, the average segregation in the test section x_A/X_A, the solid volume fractions ratio in the feed X_A and the pressure drop along the test section were measured. In our numerical calculations, a gas volume fraction and one solid velocity (or one solid volume fraction) and pressure at the inlet at any arbitrary point in the line are needed. Since such data were not given in the cited experiment, reasonable values for initial pressure and inlet gas volume fraction were chosen.

The effect of system pressure on the pressure drop using models A and B is not significant in the low-pressure range. However, model C, the relative velocity model, shows a significant effect of system pressure

even in a narrow range of pressure variation of 1.03×10^5 N/sq m to 1.72×10^5 N/sq m. All models show a sensitivity due to the initial gas volume fractions of 0.995 to 0.999. A reasonable initial pressure of 1.137×10^5 N/sq m (slightly greater than atmospheric pressure) was chosen. For a solid mass flow rate of 33.46 kg/m^{2}sec the predicted values using the relative velocity model agreed with experimental values at a volumetric concentration of $\varepsilon_{g_1} = 0.9973$. This value for initial void fraction is different using the other two models. All three models compared reasonably well with Nakamura's and Capes' experimental data. Typical comparisons of pressure drop with the experiment are shown in Figure 7 using the relative velocity model. The relative velocity model shows slightly better agreement with Nakamura's and Capes' segregation data than the other models. Figure 8 shows a comparison of the particle segregation with their experiment using the relative velocity model. The deviation is due to the neglect of binary collisional friction forces in our model. An independent measurement of such friction forces is needed to refine the model.

NOMENCLATURE

C_{DA}	=	The drag coefficient for solid phase A
C_{DB}	=	The drag coefficient for solid phase B
D	=	Diameter of the conveying pipe
d_A	=	Diameter of particles A
d_B	=	Diameter of particles B
f_A	=	Drag force per unit volume of solid phase A
f_B	=	Drag force per unit volume of solid phase B
f_g	=	Gas wall friction factor
f_w	=	Gas wall friction force
L	=	Length of the conveying pipe
P	=	Pressure
P_1	=	The initial pressure
Re_A	=	Solid phase A Reynolds number
Re_B	=	Solid phase B Reynolds number
Re_g	=	Gas Reynolds number
v_A	=	Solid A phase velocity
v_B	=	Solid B phase velocity
v_g	=	Gas velocity
W_s	=	Solid mass flow rate
x	=	Coordinate parallel to flow direction
X_A	=	Solid volume fraction ratio of solid A phase in the feed

Greek Letters

ε_A	=	Volume fraction of solid A phase
ε_B	=	Volume fraction of solid B phase
ε_g	=	Gas volume fraction
ε_{gl}	=	Initial gas volume fraction
μ_g	=	Viscosity of the gas
ρ_A	=	Density of the solid particle A
ρ_B	=	Density of the solid particle B
ρ_g	=	Density of the gas
ρ_{gl}	=	Initial density of the gas

Acknowledgment:

One of the authors (D.G.) thanks the Department of Energy for partial support of this study under Contract No. DOE ET-78-G-01-3381 and also the Gas Research Institute, Grant No. GRI 5014-363-0137.

References

1. Nakamura, K. and Capes, C.E., "Vertical Pneumatic Conveying of Binary Particle Mixtures," in Fluidization Technology (Edited by D.Keairns), Vol. 2, p. 159. Hemisphere Publishing Corporation, Washington, D.C. (1976).

2. Soo, S.L., Fluid Dynamics of Multiphase Systems, Waltham, Massachusetts, Blaisdell Publishing Company (1967).

3. Gidaspow, D., "Fluid Particle System," in Two Phase Flow and Heat Transfer, edited by Kakac, S. and Mayinger, F., 1, 115-128 Hemisphere Publishing Corporation (1977).

4. Gidaspow, D. "Hyperbolic Compressible Two-Phase Flow Equations Based on Stationary Principles and the Fick's Law," in Two Phase Transport and Reactor Safety. Edited by Kakac, S. and Vezıroglu, T.N. 283-298 Hemisphere Publishing Corporation (1978).

5. Arastoopour, H., "Hydrodynamic Analysis of Solids Transport," PhD Thesis, Illinois Institute of Technology, Chicago, Illinois (1978).

6. Handbook of Natural Gas Engineering, McGraw-Hill Book Company, Inc. New York (1959).

7. Lin, D., M.S. Thesis, Illinois Institute of Technology, Chicago, Illinois (1978).

8. Shook, C.A. and Masliyah, J.H., "Flow of a Slurry Through a Venturi Meter," Can. J. Chem. Eng. 52, 228-33 (1974).

9. Chandok, S.S. and Pei, D.C.T., "Particle Dynamics in Solid-Gas Flow in a Vertical Pipe," First International Conference on the Pneumatic Transport of Solids in Pipe, Spt. 6-8 (1971).

10. Arastoopour, H. and Gidaspow, D., "Analysis of IGT Pneumatic Conveying Data and Fast Fluidization Using a Thermodynamic Model," Powder Technology 22, 77-87 (1979).

11. Arastoopour, H. and Gidaspow, D. on "Two Phase Flow Fundamentals," in Two Phase Transport and Reactor Safety 1, 133-158. Hemisphere Publishing Corporation (1978).

12. Yang, W.C., "Study on Segregation Modeling of Particles in Dilute Phase Vertical Pneumatic Transport Lines," The Fourth Internal Conference on the Pneumatic Transport of Solids in Pipes, June 26-28 (1978).

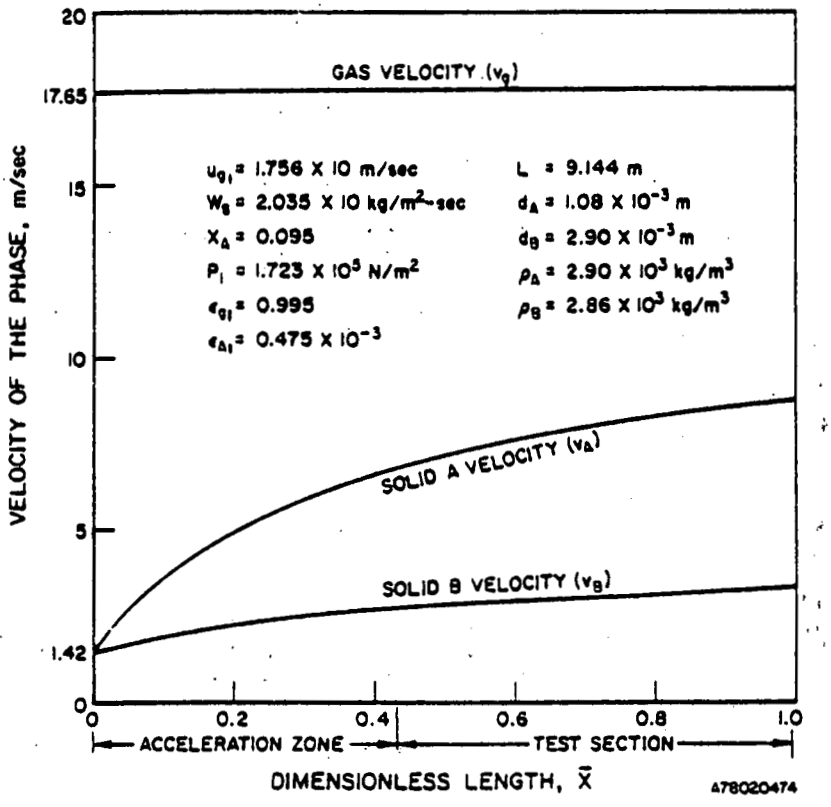

Figure 1. Phase Velocities for Solids-Gas Flow Through a Vertical Pipe Using the Relative Velocity Model

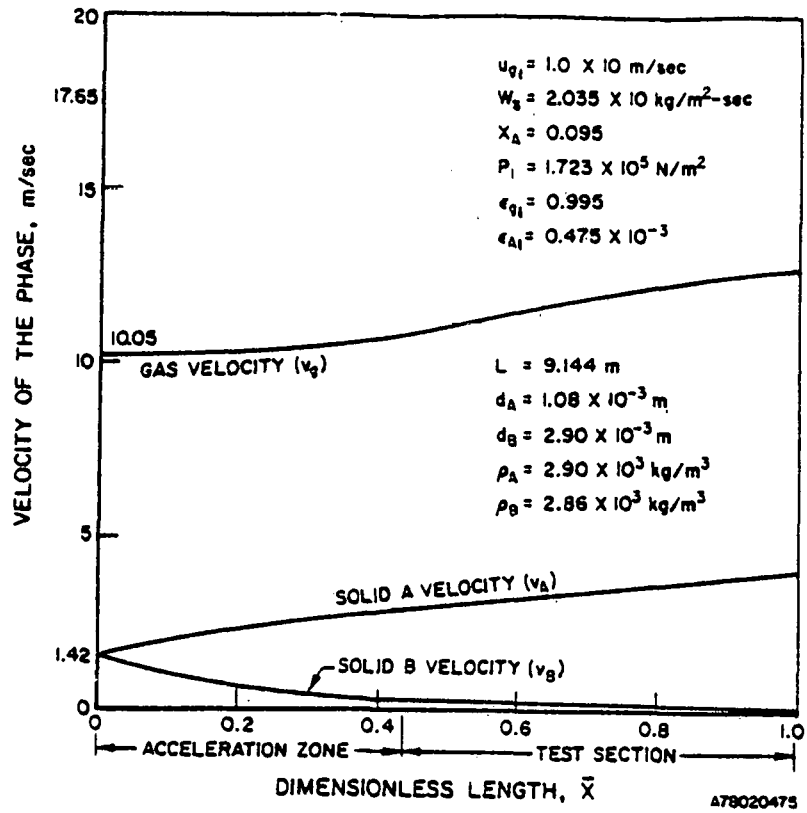

Figure 2. Phase Velocities for Solids-Gas Flow Through a Vertical Pipe Using the Relative Velocity Model When the Superficial Gas Velocity Approaches the Choking Velocity

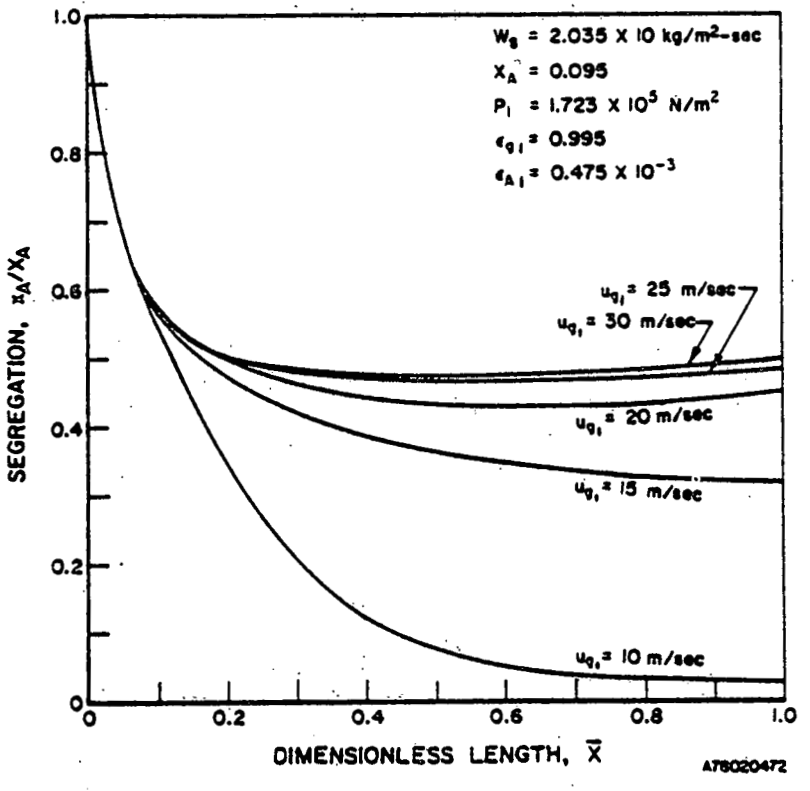

Figure 3. The Effect of Initial Superficial Gas Velocity on the Segregation of Solid Mixtures Through a Vertical Tube Calculated Using the Relative Velocity Model

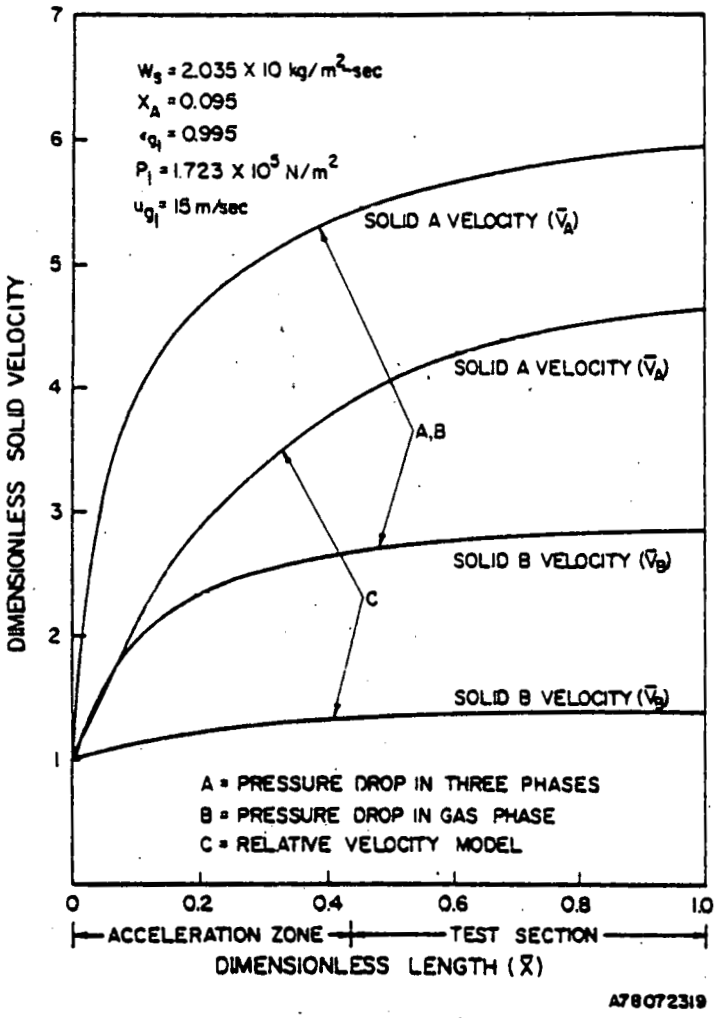

Figure 4. A Comparison of Dimensionless Solid Velocities Through a Vertical Pipe Calculated Using Three Unequal Velocity Models

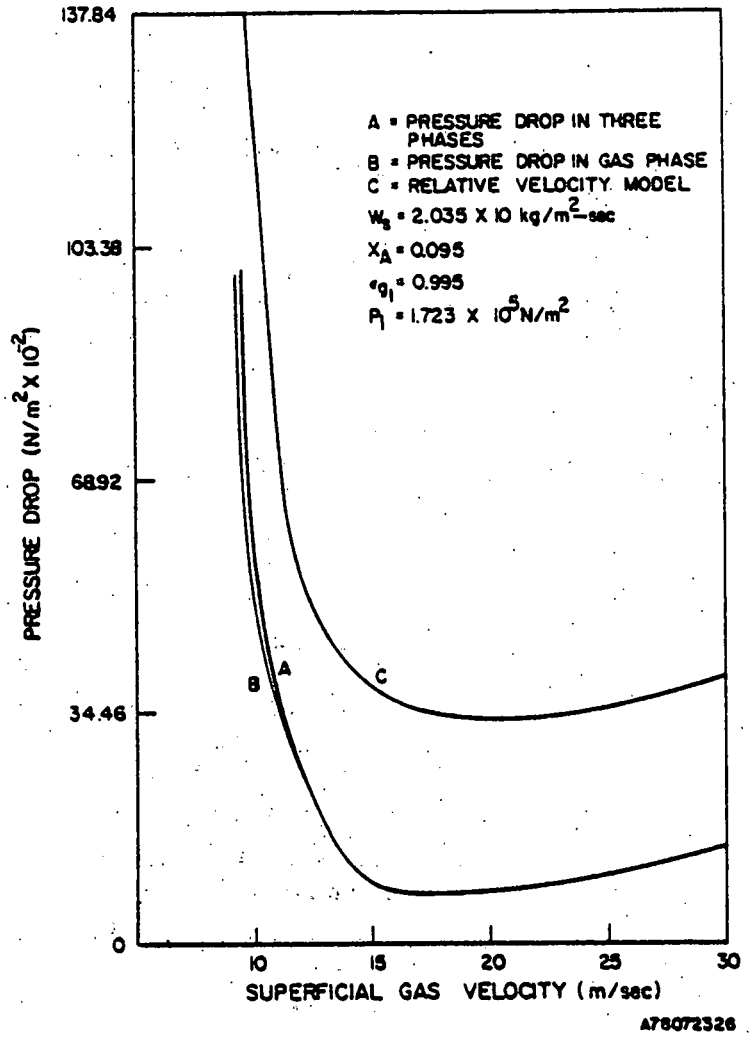

Figure 5. The Effect of Superficial Gas Velocity on the Pressure Drop for Flow of a Gas-Solids Mixture Through a Vertical Pipe Calculated Using Three Unequal Velocity Models

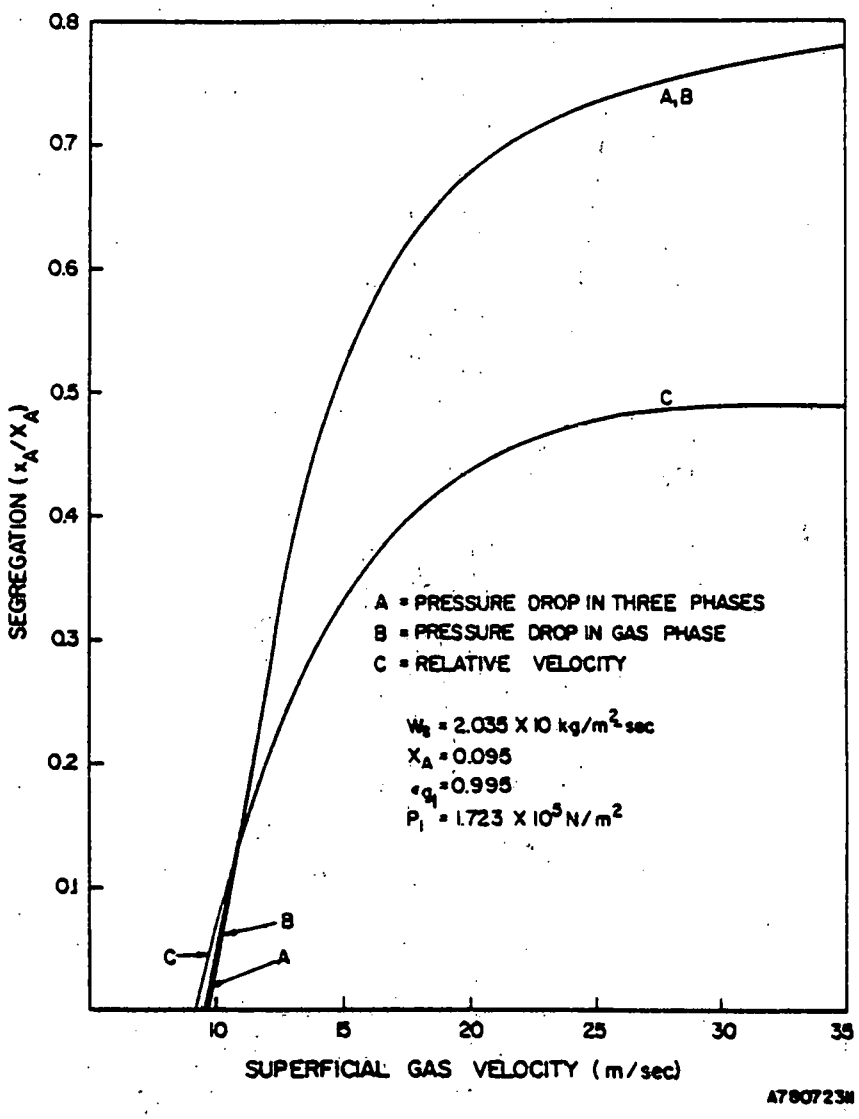

Figure 6. The Effect of Superficial Gas Velocity on Segregation of the Solids Mixture Through a Vertical Pipe Calculated Using Three Unequal Velocity Models

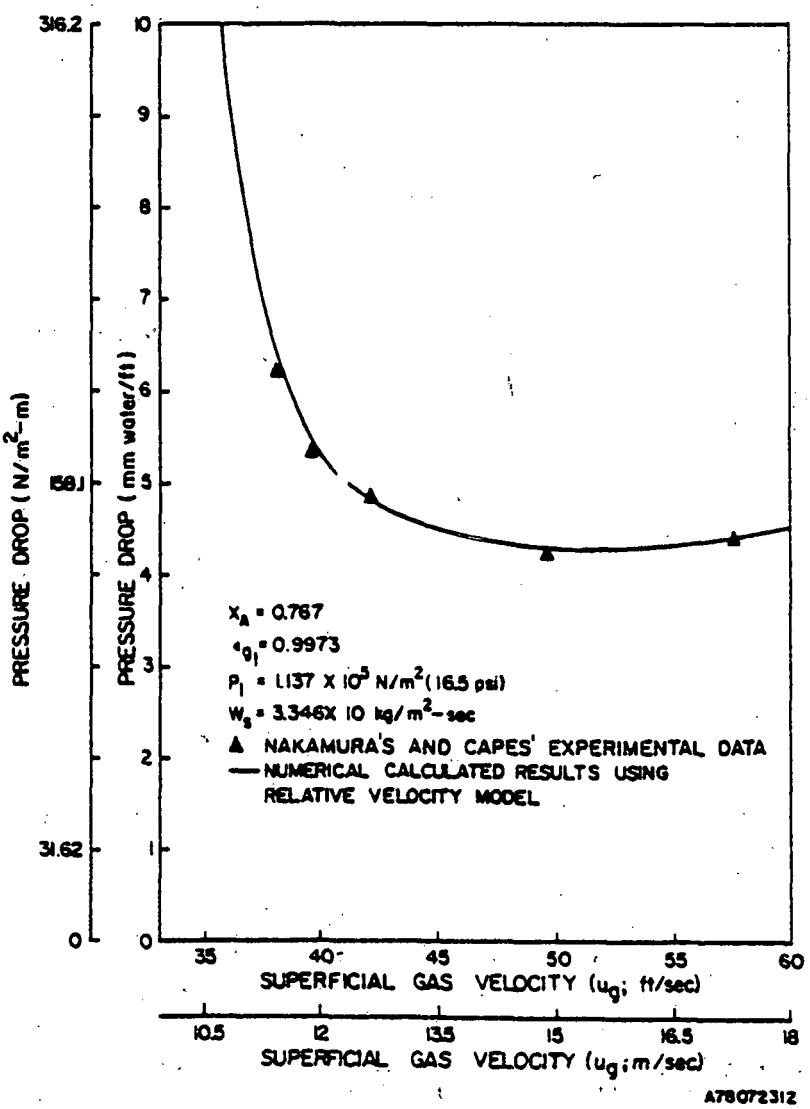

Figure 7. A Comparison of Nakamura's and Capes' Experimental Data [1] With a Numerical Solution for a Solids-Gas Flow Through a Vertical Pipe Using the Relative Velocity Model for an Inlet Gas Volume Fraction of 0.9973 and Solid Mass Flow Rate of 33.46 kg/sq m-sec

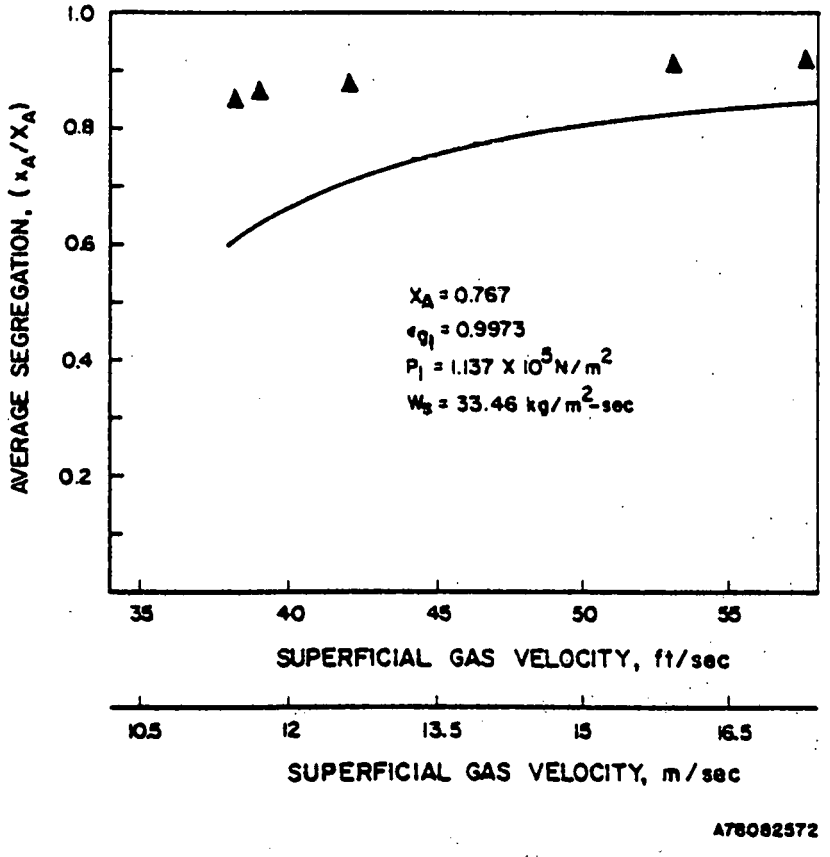

Figure 8. A Comparison in Segregation of Nakamura's and Capes' Experimental Data [1] With a Numerical Solution for a Solids-Gas Flow Through a Vertical Pipe Using the Relative Velocity Model for an Inlet Gas Volume Fraction of 0.9973 and Solid Mass Flow Rate of 33.46 kg/sq m-sec

Vertical Pneumatic Conveying Using Four Hydrodynamic Models

Hamid Arastoopour

Institute of Gas Technology, Chicago, Illinois 60616

Dimitri Gidaspow*

Department of Chemical Engineering, Illinois Institute of Technology, Chicago, Illinois 60616

Pressure drop in vertical transport of solids was calculated using four hydrodynamic models previously proposed. The calculations were done using literature correlations of friction factors. Three of the models predict a minimum in pressure drop vs. superficial gas velocity. The three models—a relative velocity model, a model with pressure drop in the gas and solid phases, and a model with a pressure drop in the gas phase only—predict a choking behavior associated with flow reversal of particles. The relative velocity model compares well with Zenz's experimental data with a fixed inlet volume fraction.

Background of Hydrodynamic Models

A hydrodynamic approach to fluidization was started by Davidson in 1961. He analyzed single bubble motion in an infinite fluid bed using two continuity equations and an expression for relative velocities in terms of Darcy's law for flow in porous media. Davidson assumed that the solids flow around a bubble was irrotational. This assumption (Gidaspow and Solbrig, 1976) can be justified based on the mixture momentum equation. It can also be shown (Gidaspow and Solbrig, 1976) that the use of Darcy's law and the mixture momentum equation is in the limit equivalent to the use of two separate phase momentum

balances. A year after Davidson's solution, Jackson (1963) formulated the more general equations of motion. Later, Jackson (1971) reviewed his work and that of others.

In the last few years interest in hydrodynamic modeling was renewed due to the energy crisis (Gidaspow and Solbrig, 1976). When an attempt was made to solve the hydrodynamic models similar to those presented by Jackson numerically on high-speed computers, it was found that the differential equations are ill-posed as an initial value problem (Gidaspow, 1974; Lyczkowski et al., 1978). According to a theorem in the literature (Lax, 1958) it is impossible to find a numerically stable finite difference technique to solve such a set of equations. Several solutions to this dilemma are possible.

One approach is to use a set of equations which neglects interaction of inertia between the gas and the particles. One simply writes Newton's second law of motion for particles. Such a set of equations had been used by aerodynamicists. It is not ill-posed.

The second approach is to derive an equation of relative motion using the principles of nonequilibrium thermodynamics. This approach was described by Gidaspow (1978).

The third approach is to modify Jackson's equations by dropping and adding proper terms so as to remedy the ill-posedness problem. This was done by a Systems, Science and Software group in a paper presented in December 1976 (Pritchett et al., 1976).

For steady-state problems mathematical difficulties do not arise. In the two-phase flow literature there are a number of problems solved using two continuity and two momentum equations. One of the earliest and best described problems is that of flow through a nozzle (Soo, 1967). For pneumatic transport Nakamura and Capes (1973) considered a similar approach.

Two Velocity Models

Vertical pneumatic conveying of solids of a reasonably uniform size can be described by means of one-dimensional, isothermal steady-state mass and momentum balances. The one-dimensional approximation is probably better for vertical than for horizontal transport due to segregation and settling in horizontal flow at low gas velocities. The isothermal assumption is a good approximation for dispersed flow due to good heat transfer to the wall and low rates of heat generation by friction. The assumption of a steady-state discards any fluctuations, such as those that occur in slug flow.

The four differential equations can be written as the two continuity equations with no phase changes and a mixture momemtum equation, plus a fourth equation which differs from model to model. The common equations are as follows.

fluid continuity
$$\frac{d}{dx}[\epsilon\rho_g v_g] = 0 \tag{1}$$

solid continuity
$$\frac{d}{dx}[(1-\epsilon)\rho_s v_s] = 0 \tag{2}$$

mixture momentum
$$(1-\epsilon)\rho_s v_s \frac{dv_s}{dx} + \epsilon\rho_g v_g \frac{dv_g}{dx} + (\rho_s(1-\epsilon) + \rho_g\epsilon)g \sin\theta = -\frac{dP}{dx} - f_w \tag{3}$$

We want to determine v_g, v_s, ϵ, and P. Therefore, we need one more equation. The four different momentum balances used in the literature are: case A, pressure drop in both solid and fluid phases (annular flow model) (e.g., Nakamura and Capes, 1973)

$$\rho_s v_s \frac{dv_s}{dx} + \frac{dP}{dx} = f_s - \rho_s g \sin\theta \tag{4}$$

case B, pressure drop in fluid phase only (e.g., Soo, 1967)

$$\rho_s v_s \frac{dv_s}{dx} = f_s - \rho_s g \sin\theta \tag{5}$$

case C, relative velocity (Gidaspow, 1978)

$$-\frac{1}{2}\frac{d}{dx}(v_g - v_s)^2 = \frac{f_s}{\rho_s} - g \sin\theta \tag{6}$$

case D, partial pressure drop in both phases (e.g., Deich et al., 1974)

$$\rho_s v_s \frac{dv_s}{dx} - \frac{P}{(1-\epsilon)}\frac{d\epsilon}{dx} + \frac{dP}{dx} = f_s - \rho_s g \sin\theta \tag{7}$$

In the above equations θ is the angle between the pipe axis with a horizontal line, f_w and f_s are wall friction and drag force per unit volume of particles, respectively, and f_w, the frictional force between the gas and the wall, can be expressed by means of the usual Fanning-type equation as

$$f_w = \frac{f_g \rho_g v_g^2}{2D} \tag{8}$$

where f_g, the friction factor, is a function of gas Reynolds number and relative roughness of the pipe. The pipe was assumed smooth in our calculation. Therefore, f_g is a function only of the gas Reynolds number. For the lower Reynolds number, the friction factor can be obtained from the empirical Blasius formula

$$f_g = \frac{0.316}{Re_g^{1/4}} \qquad Re_g < 100\,000 \tag{9}$$

For higher gas Reynolds numbers, the friction factor can be obtained from the following expression ("Handbook of Natural Gas Engineering", 1959)

$$\frac{1}{\sqrt{f_g}} = 2 \log (Re_g\sqrt{f_g}) - 0.8 \tag{10}$$

The effect of particles on wall friction was neglected, since primarily dilute phase transport is considered.

Drag Force. The drag force on a single spherical particle in an infinite fluid is usually expressed in terms of a drag coefficient C_{Ds} as

$$F_D = C_{Ds}(\pi d^2/4)\rho_f v_r^2/2 \tag{11}$$

where v_r is the relative velocity between the particle and the fluid. Soo (1967) summarizes the dependence of the drag coefficient on the Reynolds number. To take into account the effect of concentration of particles in sedimentation or fluidization, Richardson and Zaki (1954) showed that the drag force per unit weight of particles between spherical solids and fluid mixtures can be expressed as

$$F_D = 3C_{Ds}/4 \frac{\rho_f(v_f - v_s)^2}{d(\rho_s - \rho_f)}\epsilon^{-2.65} \tag{12}$$

Equation 12 was obtained from eq 11 by dividing by the effective weight of the particles and by including the empirical dependence on void fractions. In Richardson and Zaki's (1954) correlation, a suspension velocity is used. It is related to the relative velocity by means of the relation suspension velocity = $(v_f - v_s)\epsilon$. Then in terms of this suspension velocity the exponent on the void fractions in eq 12 becomes −4.65 (Wen and Galli, 1971). As shown by

Soo (1967), the relation of suspension velocity to relative velocity is valid for settling of incompressible particles in an incompressible fluid. In the momentum equations, f_s, the drag force exerted by fluid on the particles per unit volume of particles, can be written as

$$f_s = 3\,C_{Ds}/4\frac{\rho_f(v_f - v_s)^2}{d}\epsilon^{-2.65} \tag{13}$$

The above correlation for the drag force is valid for spherical particles, where d is the particle diameter and C_{Ds} is a drag coefficient. The quantity C_{Ds} can be evaluated from known quantities. The drag coefficient can be related to the Reynolds number (Rowe and Henwood, 1961) by means of the relations

$$C_{Ds} = \frac{24}{Re_s}(1 + 0.15\,Re_s^{0.687}) \qquad Re_s < 1000 \tag{14}$$

$$C_{Ds} = 0.44 \qquad Re_s > 1000 \tag{15}$$

where

$$Re_s = \epsilon\,\rho_f d(v_f - v_s)/\mu_f \tag{16}$$

and μ_f is the viscosity of the fluid.

In Gidaspow's (1978) analysis of fluidization the friction coefficient is

$$\beta = f_s/[\rho_s(v_f - v_s)] \tag{17}$$

It can also be easily related to Soo's (1967) time constant F. For a more concentrated mixture than considered here, f_s is related to volume fractions through the Ergun equation as, for example, given by Soo (1976, p 368). The friction coefficient for such a case is given by

$$\beta = \frac{150(1 - \epsilon)\mu_f}{\rho_s\epsilon^2 d^2} \tag{18}$$

As discussed by Soo (1967), this packed bed friction factor is considerably larger in numerical value than that obtained from eq 13 with use of Stokes' law and a value of void fraction raised to a power. The principal advantage of the form (18) is, however, the presence of the factor $(1 - \epsilon)$. The presence of such a factor will make the drag or friction vanish for a bubble. This is a desirable feature, because bubbles are known to move in nearly potential flow. Equation 6 integrated over a bubble gives roughly the bubble velocity. With f_s equal to zero in eq 6 and for a vertical pipe integration over the region of zero f_s, that is, the bubble yields

$$v_s - v_g = \pm\sqrt{2gx + \text{constant}} \tag{19}$$

The constant is evaluated from the condition that at the tip of the bubble, we have minimum fluidization velocity. This gives

$$v_{\text{bubble}} = v_g + \sqrt{2gD_{\text{bubble}} + U_{mf}^2} \tag{20}$$

The comparison to experimental bubble velocities is good in view of the drastic assumptions made in the integration.

Analysis of Four Models

The two continuity equations, a mixture momentum equation, plus a fourth equation which is different for different cases are the four sets of four nonlinear first-order differential equations which describe the system. The continuity equations (1) and (2) can be expressed as algebraic equations in terms of constant inlet solids flow rate, w_s, and inlet gas flow rate, w_g, as

$$(1 - \epsilon)v_s\rho_s = (1 - \epsilon_1)v_{s_1}\rho_s = w_s \tag{21}$$

$$\epsilon\,\rho_g v_g = \epsilon_1\rho_{g_1}v_{g_1} = w_g \tag{22}$$

The ideal gas equation of state is assumed to hold for the gas phase. The solid phase is incompressible. The governing equations are dimensionalized using the following definitions

$$\bar{v}_g = \frac{v_g}{v_{g_1}};\quad \bar{v}_s = \frac{v_s}{v_{s_1}};\quad \bar{x} = \frac{x}{L};\quad \bar{P} = \frac{P}{P_1};\quad \bar{\epsilon} = \frac{\epsilon}{\epsilon_1};$$

$$R = \frac{\rho_s}{\rho_{g_1}};\quad s = \frac{v_{s_1}}{v_{g_1}};\quad C = \frac{P_1 g}{\rho_{g_1}v_{g_1}^2};\quad F = \frac{gL}{v_{g_1}^2};$$

$$G = \frac{3}{4}C_{Ds}\frac{L}{d}(\epsilon_1)^{-2.7}$$

The system of equations can be expressed in the form of an initial value problem

$$\frac{d\vec{y}}{d\vec{x}} = f(\vec{y}) \tag{23}$$

$$\vec{y}(0) = \vec{y}_0 \tag{24}$$

For a numerical integration, the continuity and the mixture momentum equation can be written as

$$\bar{\epsilon} = \frac{1}{\epsilon_1}\left(1 - \frac{1 - \epsilon_1}{\bar{v}_s}\right) \tag{25}$$

$$\bar{v}_g = \frac{1}{\bar{\epsilon}\bar{P}} \tag{26}$$

$$d\bar{P}/d\bar{x} = \left\{\left[\bar{P}(1 - \epsilon_1)(1 - Rs^2\bar{\epsilon}^2\bar{v}_s^2\bar{P})\frac{(d\bar{v}_s}{d\bar{x}}\right] - [\bar{P}^2\bar{\epsilon}^2\bar{v}_s^2(-f_g L\bar{v}_g^2\bar{P}/2D - F(R(1 - \epsilon_1\bar{\epsilon}) + \epsilon_1\bar{P}\bar{\epsilon}))]\right\} \Big/ \{\bar{v}_s^2\bar{\epsilon}(C\bar{\epsilon}\bar{P}^2 - \epsilon_1)\} \tag{27}$$

The above form of the equations enables us to make a qualitative analysis of certain special characteristics of the physical process. The right side of eq 27 shows that the pressure drop can become unbounded when the denominator goes to zero. Mathematically the denominator vanishes at three different points.

Case I: Zero Solids Velocity, $v_s = 0$. This occurs when the solids are no longer transported up the pipe despite constant input. In such a situation no steady state can exist. It is a point where the solids will accumulate and block the pipe. This condition is thus related to the second singular point below.

Case II: Zero Voids, $\epsilon = 0$. This is the point where the solid concentration is 1. The pipe may be blocked by the solid or slugging may occur. The solids are then carried up by the gas slugs, as in a slugging fluidized bed. Mathematically, there is no steady-state solution. Cases I and II are related to the phenomenon of choking in vertical pneumatic transport.

Case III: Sonic Limit, $C\bar{\epsilon}\bar{P}^2 = \epsilon_1$. This expression gives an isothermal sonic velocity reduced by the square root of void fractions

$$U_g = \epsilon v_g = \sqrt{\frac{\epsilon R_g T}{M_g}} \tag{28}$$

This limit is close to the usual choking condition in single phase pipe flow.

Analysis of the second momentum equation gives the following information for the four different cases.

Pressure Drops in Both Phases (Case A). The dimensionless differential equation for solids velocity is

$$d\bar{v}_s/d\bar{x} = [(G(\bar{v}_g - s\bar{v}_s)|\bar{v}_g - s\bar{v}_s|\bar{\epsilon}^{-1.7}\bar{v}_s\bar{P} - FR\bar{v}_s\bar{\epsilon}) \times (C\bar{\epsilon}\bar{P}^2 - \epsilon_1) - Cf_gL\bar{v}_s/2D - CF\bar{v}_s(R(1 - \epsilon_1\bar{\epsilon}) + \epsilon_1\bar{P}\bar{\epsilon})/\bar{v}_g^2]/[Rs^2\bar{v}_s^2\bar{\epsilon}\epsilon_1(C\bar{\epsilon}^2\bar{P}^2 - 1) + C\bar{P}(1 - \epsilon_1\bar{\epsilon})] \quad (29)$$

This model does not have any additional critical conditions.

Giot and Fritte (1972), Capes and Nakamura (1973), and Yousfi and Gau (1974) used this annular flow model in analyzing their two-phase flow situations. Also, Shook and Masliyah (1974) and Arastoopour and Gidaspow (1978) used this type of model to evaluate discharge coefficients for flow of a slurry through a venturimeter. It is particularly popular in the literature in gas–liquid two-phase flow.

No Pressure Drop in Solids Phase (Case B). The dimensionless differential equation for solid velocity suitable and necessary for a Runge–Kutta numerical calculation can be written as

$$\frac{d\bar{v}_s}{d\bar{x}} = \frac{G}{s^2}\left[\frac{\bar{P}\bar{\epsilon}^{-2.7}}{\bar{v}_sR}(\bar{v}_g - s\bar{v}_s)|\bar{v}_g - s\bar{v}_s|\right] - F/s^2\bar{v}_s \quad (30)$$

Substituting the above equation for solid velocity into the mixture momentum equation, the differential pressure drop can be rearranged to show the individual contributions due to acceleration, drag, wall frictions, and gravity.

$$\frac{d\bar{P}}{d\bar{x}} = \frac{1}{C}\Bigg\{\underbrace{-\epsilon_1\bar{P}\bar{\epsilon}\bar{v}_g\frac{d\bar{v}_g}{d\bar{x}}}_{\text{gas momentum}} - \underbrace{RG\bar{\epsilon}^{-2.7}\bar{P}(1 - \epsilon_1\bar{\epsilon})(\bar{v}_g - s\bar{v}_s)|\bar{v}_g - s\bar{v}_s|}_{\text{drag force}} - \underbrace{\frac{f_gL}{2D}\bar{v}_g^2\bar{P}}_{\text{wall friction}} - \underbrace{F\epsilon_1\bar{\epsilon}}_{\text{gas gravity}}\Bigg\} \quad (31)$$

This model also does not show any further limitation for critical flow beyond those given by the mixture momentum equation. This is the oldest model in the two-phase flow literature. It was successfully applied to dilute particle flow by many investigators, the principal being Soo (1967) and Rudinger and Chang (1964). Unlike the annular model it is well posed as an initial value problem (Lyczkowski et al., 1978; Gidaspow, 1977).

Relative Velocity Equation (Case C). The relative velocity equation was derived by Gidaspow (1978) by using an entropy production principle. It was successfully applied to a steady, one-dimensional flow through a venturi by Arastoopour and Gidaspow (1978). The dimensionless differential equation for solids velocity is

$$d\bar{v}_s/d\bar{x} = [\epsilon_1\bar{v}_s^2\bar{P}(f_gL\bar{v}_g^2\bar{P}/2D + F(R(1 - \epsilon_1\bar{\epsilon}) + \epsilon_1\bar{\epsilon}\bar{P}) - G\bar{\epsilon}^{-2.7}\bar{P}(\bar{v}_g - s\bar{v}_s)/R + F/(\bar{v}_g - s\bar{v}_s)(C\epsilon_1\bar{P} - \epsilon_1))]/[s\epsilon_1^2\bar{\epsilon}\bar{v}_s^2(\epsilon_1 - C\bar{\epsilon}\bar{P}^2 + (1 - \epsilon_1)Rs) - (1 - \epsilon_1)C\bar{P}] \quad (32)$$

The above expression for solids velocity gradient blows up at a point where its denominator is zero and results in a further limitation for possible flows. The critical gas velocity can be written as

$$v_g = \frac{W_s}{\rho_s\epsilon}\left(1 + \frac{\epsilon R_gT}{M_gv_g^2}\left(1 + \frac{W_s}{W_g}\right)\right) \quad (33)$$

where $(R_gT/M_g)^{1/2}$ is the isothermal sonic velocity of gas, which is of the same order of magnitude as the known adiabatic sonic velocity.

Partial Pressure Drops in Both Cases (Case D). The dimensionless differential equation for the solid velocity can be written as

$$d\bar{v}_s/d\bar{x} = [(G(\bar{v}_g - s\bar{v}_s)|\bar{v}_g - s\bar{v}_s|\bar{\epsilon}^{-1.7}\bar{v}_s\bar{P} - FR\bar{v}_s\bar{\epsilon}) \times (C\bar{\epsilon}\bar{P}^2 - \epsilon_1) - Cf_gL\bar{v}_s/2D - CF\bar{v}_s(R(1 - \sigma_1\bar{\epsilon}) + \epsilon_1\bar{\epsilon}\bar{P})/\bar{v}_g^2]/[Rs^2\bar{v}_s^2\bar{\epsilon}\epsilon_1(C\bar{\epsilon}^2\bar{P}^2 - 1) + C\bar{P}(1 - \epsilon_1\bar{\epsilon}) - \bar{\epsilon}(C\bar{\epsilon}\bar{P}^2 - \epsilon_1)] \quad (34)$$

Equating the denominator of the above expression to zero results in another condition for critical flow

$$\bar{v}_g^2 = \frac{R_gT}{M_g} \quad (35)$$

The above critical condition is the same as that obtained by Deich et al. (1974) for flow of gas and liquid through a nozzle. It is the usual isothermal sonic limit that is numerically smaller than that obtained from the mixture equation. A fifth-order Runge–Kutta method was used to obtain the numerical results with initial condition at $x = 0$; $\bar{P} = \bar{v}_s = 1$.

A Parametric Study Using the Relative Velocity Model

In order to use actual numerical values and be able to compare our calculated results with the available experimental data, the vertical lift line studied here is the same as the one used by Zenz (1949) in his experimental study of two-phase gas–solid flow through a vertical tube. The diameter of the tube was 4.45×10^{-2} m and its length was 1.12 m. The experiments were done with air and with spherical rape seed of a diameter of 1.67×10^{-3} m and density of 1098 kg/m^3 as the solid phase. Several other experimental data sets for gas–solid flow through a tube were also studied, such as those by Farbar (1949), Mehta et al. (1957), Capes and Nakamura (1973), and Hariu and Molstad (1949). In all these experimental studies the gas and solid mass flow rates, in addition to the pressure drop, have been measured. In order to compare the data to calculations, a solid concentration (solid volume fraction) or a solid velocity at the inlet or at some arbitrary point along the tube is needed. Only Hariu and Molstad (1949) measured the total mass of the solid in the tube as a result of which they obtained the averaged solid velocity that could be useful in analyzing the process. It is also necessary to measure the actual inlet pressure or the pressure at any arbitrary point along the line.

The solid volume fraction, the pressure drop, and the solid and gas velocities were calculated using the four different models. Figure 1 shows typical solid and gas velocity plots and solid volumetric concentrations along the height of a vertical tube using the relative velocity model at a solid mass flow rate of 62.44 kg/m^2-s and at an initial void fraction and pressure of 0.9 and 26.4×10^4 N/m^2, respectively. The superficial gas velocity was 9.15 m/s. The gas velocity decreases as the solid particles accelerate; the solid volume fraction therefore decreases due to the increase in solid velocity at a constant solid mass flow rate throughout the vertical line. The effect of the inlet conditions was studied using the relative velocity model to find out the effect of the changes of the initial values on predicting the other properties of the gas–solid flow in the lift line at a constant solid mass flow rate of 62.44 kg/m^2-s. The effect of the initial gas velocity was at the initial pressure and volumetric concentration of P_1

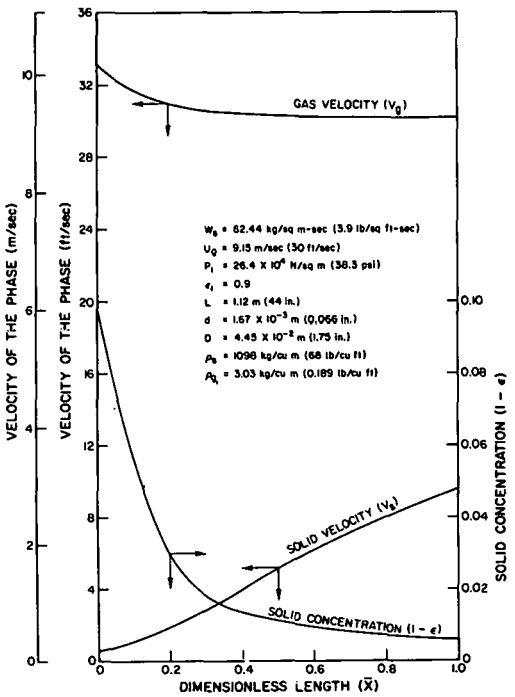

Figure 1. Solids volume fraction and phase velocities for solid–gas flow through a vertical tube using the relative velocity model.

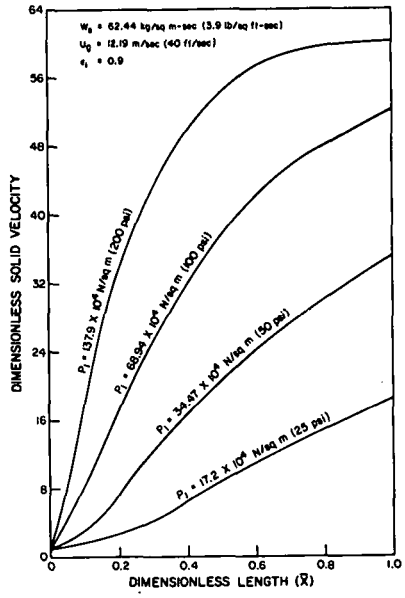

Figure 2. The effect of initial pressure on the solid velocity through a vertical tube calculated using the relative velocity model.

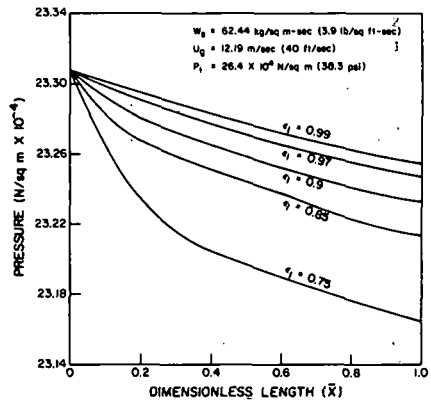

Figure 3. Pressure variation through a vertical tube at different initial solid volumetric concentrations calculated using the relative velocity model.

$= 26.4 \times 10^4$ N/m^2 and $\epsilon_1 = 0.9$, respectively. As physically expected, lower initial gas velocity results in lower solid velocities through the lift line.

At a very low gas velocity when the gas cannot accelerate the particle, the gas velocity increases due to the decrease in volumetric gas concentration and constant gas mass flow rates. For high enough gas velocities, such as U_g greater than 9 m/s, the pressure drop increases with increasing initial gas velocities. This behavior is the same as in single phase flow. But for the lower velocities, such as U_g less than 9 m/s, it is reversed; the pressure drop increases with decreasing initial gas velocities. The rate of change of the pressure drop with respect to the initial gas velocity is much higher for lower gas velocities (in our case, U_g less than 9 m/s) than for higher velocities (in our case, U_g greater than 9 m/s).

Figure 2 shows the effect of the initial pressure on the solid velocity through the vertical tube. The relative velocity model shows that at higher pressures the solid particles accelerate more and, as a result of this phenomenon, the length of the acceleration zone decreases and the solid concentrations are lower than for the case of lower pressures. This result is expected based on the physical behavior of the system. At 12.2 m/s superficial velocity for a higher pressure range of about 60×10^4 N/m^2 or more, the value of the pressure drop increases with increasing initial pressure. At $P_1 = 68.94 \times 10^4$ and 137.9×10^4 N/m^2, the calculated values of the pressure drops were 502.57 and 743.9 N/m^2, respectively. The length of the acceleration zone decreases, thereby increasing the rate of acceleration of the particles at the higher initial pressure.

The effect of the inlet solid volume fraction was computed. This computation showed that the initial volumetric concentration of the solid contributed in predicting the other properties of the vertical flow of gas and solid. It also proves the necessity of measuring the concentration of the phases in any experimental analysis. Figure 3 shows the increase in the pressure drop throughout the lift line with increasing solid volume fraction, as physically expected. On the other hand, the pressure drop in the gas phase only model shows the opposite trend; that is, the pressure drop increases with decreasing solid volumetric concentration. This could be due to the higher gas momentum term in the momentum equation. Perhaps other essential factors should be considered in this model such as the relative velocity term (Soo, 1976) or the added mass term (Lamb, 1932). The different initial solid volume fractions result in different initial solid velocities. Although the relative increase in the solid velocity is higher for lower initial solid velocity, the lower initial solid velocities end up with lower final solid velocities in the acceleration zone of the vertical tube. A complete parametric study using the relative velocity model has been presented by Arastoopour (1978).

Numerical Comparison of Four Models

The calculated pressure drop, the gas and solid velocities, and the volumetric concentrations were compared with each other using the different models for flow of air and spherical rape seed mixture through a vertical tube. The vertical line and the gas–solid materials are the same as those used by Zenz (1949). The solid mass flow rate and the initial pressure are 62.44 kg/m^2-s and 26.4×10^4 N/m^2, respectively. The initial superficial gas velocity is U_g = 9.15 m/s with an assumed inlet volumetric concentration of $\epsilon_1 = 0.9$. Figure 4 shows the calculated solid volume

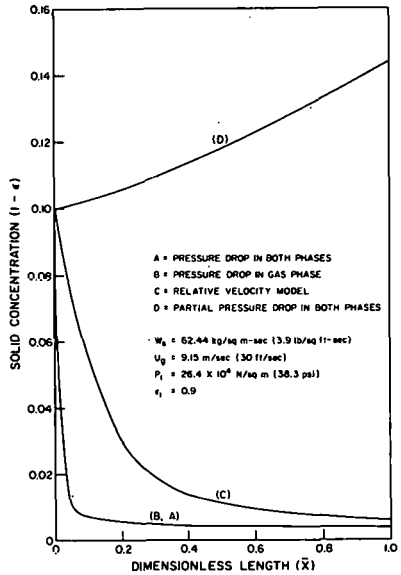

Figure 4. A comparison of solids volumetric concentration through a vertical tube calculated with four unequal velocity models.

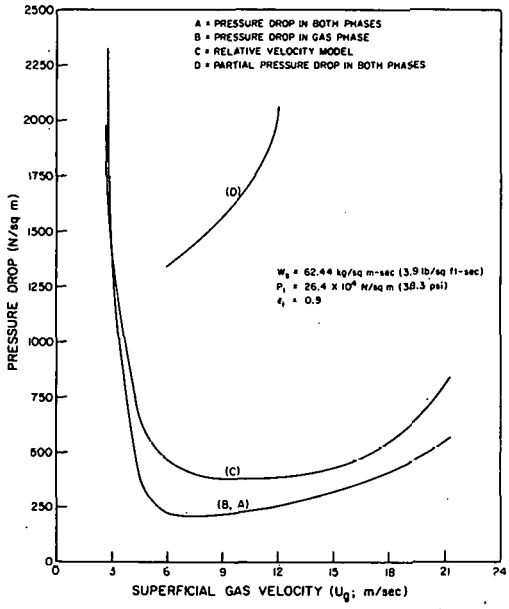

Figure 5. The effect of superficial gas velocity on the pressure drop for flow of a gas–solid mixture through a vertical tube calculated using four unequal velocity models.

fraction using the different models. Cases A, B, and C show that the solid volumetric concentration decreases through the vertical line. This is consistent with Zenz's experimental results (1949). Case D, the partial pressure drop in both phases model, shows an increase in the solid volume fraction and indicates that the solid particles decelerate through the lift line, which is not in agreement with Zenz's experimental observations. Cases B and A, the pressure drop in one and in both phases, predict the same values for the solids volume fraction through the line due to the low concentration of the particles in the mixture. They also predict a lower exit solid volume fraction than the relative velocity equation model. Case C predicts a gradual decrease in solid volumetric concentration while cases A and B show a sudden decrease in solid volume fraction at the entrance. This gradual change in the properties of the system using the relative velocity model indicates a distributed interaction between the phases throughout the vertical line. Due to constant mass flow rate of the particles, the solid velocity for cases A, B, and C increases through the line. In the case of the partial pressure drop in the both phases model (case D), the solid velocity unrealistically decreases through the lift line.

Choking Behavior

Figure 5 shows the pressure drop vs. the superficial gas velocity at a constant solids flow rate calculated using the four models. Three out of four models show the experimentally observed choking behavior and a minimum in pressure drop. Zenz (1949) was one of the first to obtain such a relation experimentally. The minimum in the pressure drop curve is a result of competition of forces that change with flow rate in the opposite direction, as seen by examining the mixture momentum (eq 3). At low gas flow rates, friction and velocity heads are small compared with the gravity term. The pressure drop is almost equal to the weight of the solids. The mixture momentum equation almost degenerates into the hydrostatic manometer formula. As the gas flow rate increases, the mixture becomes more dilute and the static head decreases. With a further increase in gas flow rate, friction begins to dominate and the pressure drop rises as in single phase flow. Today this phenomenon is qualitatively well understood. However, to design fluidized-bed reactors for converting coal to clean fuels, quantitative predictions are necessary. Knowlton and Bachovchin (1976) obtained such relations experimentally using Montana lignite that was used in the IGT Pilot Plant and demonstration plants. To be able to predict the pressure drop vs. gas flow rate curve uniquely, an inlet void fraction had to be specified. Knowlton and Bachovchin (1976) and others before them did not report this value.

Figure 5 shows that the three models give close to the same pressure drop curve. The values predicted by the partial pressure model are far off. The problem is caused by the extra force in the partial pressure model equal to

$$\frac{P}{1-\epsilon}\frac{d\epsilon}{dx}$$

This force becomes large due to the term $(1 - \epsilon)$ in the denominator. Cases A and B predict the same pressure drop at this particular chosen inlet solids concentration. At higher inlet solids volumetric concentrations, the two models give a different pressure drop–flow rate relation.

Comparison with Experiment

In order to compare our calculated quantities with Zenz's experiment, the same initial conditions and the same solid particles, gas, and vertical tube were used. From the experiment, the solid mass flow rate, W_s, the superficial velocity, U_g, and the pressure drop were measured. For our analysis, we needed an initial pressure and an initial solid velocity (or concentrations), in addition to the inlet gas velocity. Since such data were not given, reasonable values for initial pressure and inlet void fraction were chosen and used to predict the experimental pressure drop at a superficial gas velocity of 12 m/s across the lift line. The predicted values using the relative velocity equation model agreed with the experimental values at an initial pressure and at a volumetric concentration of $P_1 = 11.72 \times 10^4$ N/m^2 and $\epsilon_1 = 0.992$, respectively. The mass solid flow rate was 62.44 kg/m^2-s.

Selecting these values for initial pressure and void fractions, we are able to predict the other experimental results at different superficial gas velocities. Figure 6 shows the comparison of the pressure drop vs. the superficial gas velocity calculated using the relative velocity model with Zenz's experimental data. The calculated

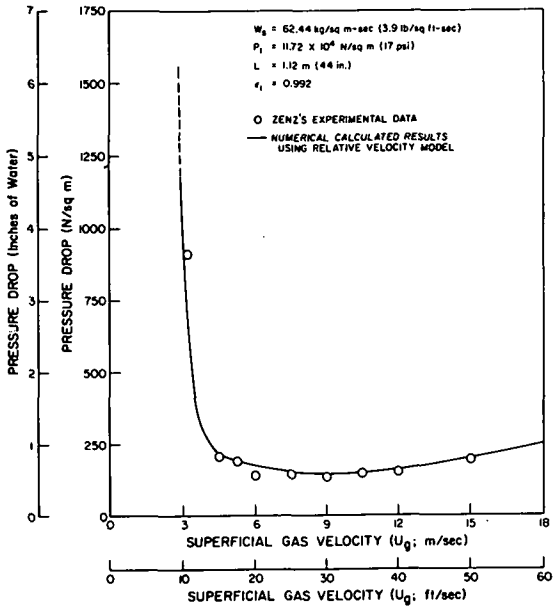

Figure 6. Comparison of Zenz's experimental data (Zenz, 1949) with a numerical solution for a cocurrent solid–gas flow through a vertical tube using the relative velocity model for an inlet void fraction of 0.992.

pressure drops are in good agreement with the experimental data. Due to the significance of the initial pressure and volumetric concentration of the solid in the mathematical analysis of the two-phase transport of the particles and fluids, the precise measurement of the above-mentioned quantities is recommended for all experimental studies of the two-phase flow.

Hariu and Molstad (1949) measured the total pressure drop in the transport of solid particles by an air stream through a vertical glass tube with an inside diameter of 6.78×10^{-3} m. Also, they measured the dispersed solid density, which enabled them to calculate the average particle velocity. This kind of measurement, average or more precisely local solid velocity, is essential because the knowledge of the solid flow rate, gas velocity, and total pressure offers no clue as to the relative values of the phases. As an example at constant gas and solid flow rate in a lift line, heavy materials will move at a slower velocity than fine, low-density powder and will have a different solid distribution in the tube.

An attempt was made to compare our calculated quantities with Hariu and Molstad's experimental data. We used the same solid particles, gas, and vertical tube, and the same initial conditions. The Ottawa Sand Type A with average particle diameter of 5×10^{-4} m and particle density of 2641.65 kg/m^3 was chosen. For our analysis, we needed an initial pressure and an initial solid velocity. Since such data were not given, reasonable values for initial pressure and inlet void fraction were chosen to predict the experimental pressure drop at a superficial gas velocity of 10.8 m/s, a solid mass flow rate of 10 kg/h, and initial pressure of $P_1 = 11.72 \times 10^4$ N/m^2. The predicted values using the relative velocity equation model for the pressure drop agreed with the experimental values at a volumetric concentration of $\epsilon_1 = 0.955$. Selecting this value for volume fraction at different solid mass flow rates, we were able to obtain reasonable values for pressure drop and average solid velocity compared with experimental values. Figure 7 shows the comparison of the pressure drop vs. the solids mass flow rate calculated using the relative velocity model with Hariu and Molstad's experimental data. The calculated pressure drops show slightly lower values than the

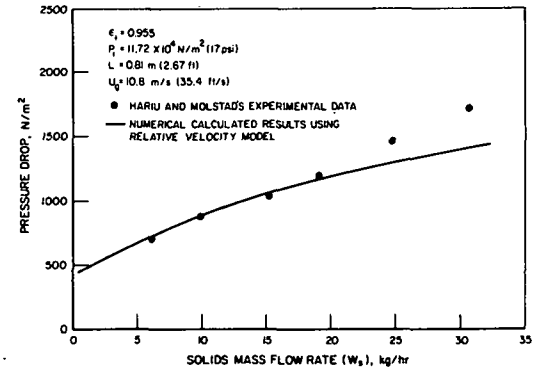

Figure 7. Comparison of the relative-velocity-model pressure drops with Hariu and Molstad's experimental data for an assumed inlet void fraction of 0.955.

experimental ones at higher solids mass flow rates. This behavior could be due to different values of initial solids volume fraction, especially at higher solids flow rates. These result in higher pressure drops through the pipe. Different initial solid volume fractions for different solid mass flow rates in the test section of the Hariu and Molstad's experiment are expected, since the air accelerates the solids after the slide valve through a section of the pipe which is located before the test section. In this portion of the pipe the solid particles of different mass flow rate move with different velocities and thus reach the test section at different velocities and void fractions. We again see that for a unique specification of the pressure drops, the inlet void fraction (or solid velocity) had to be measured.

Conclusions

1. Pressure drop and choking in dilute phase vertical pneumatic conveying can be predicted using a relative velocity hydrodynamic model. Comparison of the model to experimental data involved the use of standard drag correlations and the fitting of an inlet void fraction which was not measured.

2. Two other models used in the literature, the annular flow model and the Newton's law model with no added mass forces, also predicted the experimentally observed trends.

Nomenclature

C_{D_s} = the drag coefficient
d = diameter of the particle
D = diameter of the tube
F = Froude number, $gL/v_{g_1}^2$
f_g = gas wall friction factor
f_w = gas wall friction force
g = gravity acceleration, m/s^2
L = length of the tube
M_g = gas molecular weight
P = pressure inside the tube, N/m^2
P_1 = the initial pressure, N/m^2
$\bar{P}$ = dimensionless pressure, P/P_1
R = density ratio, ρ_s/ρ_{g_1}
R_g = perfect gas law constant
Re_g = gas Reynolds number
Re_s = solid Reynolds number
s = initial velocity ratio, v_{s_1}/v_{g_1}
T = temperature of the gas and solid
U_g = superficial gas velocity
U_{mf} = minimum fluidization velocity
v_f = fluid velocity, m/s
v_g = gas velocity, m/s
v_{g_1} = initial gas velocity, m/s
$\bar{v}_g$ = dimensionless gas velocity, v_g/v_{g_1}
v_s = solid velocity, m/s

v_{s_1} = initial solid velocity, m/s
$\bar{v}_s$ = dimensionless solid velocity, v_s/v_{s_1}
W_g = gas mass flow rate, kg/m^2-s
W_s = solid mass flow rate, kg/m^2-s
x = coordinate parallel to flow direction
$\bar{x}$ = dimensionless coordinate parallel to flow, X/L

Greek Letters

ϵ = volumetric fluid concentration
ϵ_1 = initial volumetric fluid concentration
$\bar{\epsilon}$ = dimensionless fluid concentration, ϵ/ϵ_1
θ = the angle between the tube axis and the horizontal line
μ_f = viscosity of the fluid
ρ_f = density of the fluid, kg/m^3
ρ_g = density of the gas, kg/m^3
ρ_{g_1} = initial density of the gas, kg/m^3
ρ_s = density of the solid, kg/m^3

Literature Cited

Arastoopour, H., Gidaspow, D., "Two Phase Flow Fundamentals", in "Two Phase Transport and Reactor Safety", S. Kakac and T. N. Vezlroglu, Ed., Vol. I, pp 133–158, Hemisphere Publishing Corp., 1978.
Arastoopour, H., Ph.D. Thesis, Illinois Institute of Technology, Chicago, 1978.
Capes, C. E., Nakamura, K., *Can. J. Chem. Eng.*, **51**, 31–38 (1973).
Davidson, J. F., *Trans. Inst. Chem. Eng.*, **39**, 230–232 (1961).
Delch, M. E., Danilin, V. S., Sleznev, L. I., Solomko, V. I., Talklouri, G. V., Shannon, V. K., *High Temp.* **12**(2), 299–307 (Nov 1974); (translation of *Teplofiz. Vys. Temp.*, **12** (2), 344–53 (1974) by Consultants Bureau, New York).
Farbar, L., *Ind. Eng. Chem.*, **41**, 1184–1191 (1949).
Gidaspow, D., "Hyperbolic Compressible Two-Phase Flow Equations Based on Stationary Principles and the Fick's Law", in "Two Phase Transport and Reactor Safety", S. Kakac and T. N. Vezlroglu, Ed., Vol. I, pp 283–298, Hemisphere Publishing Corp., 1978.
Gidaspow, D., "Fluid Particle Systems", in "Two Phase Flow and Heat Transfer", S. Kakac and F. Mayinger, Ed., Vol I, pp 115–128, Hemisphere Publishing Corp., 1977.
Gidaspow, D. Solbrig, C. W., "Transient Two-Phase Flow Models in Energy Production," State of the Art Paper presented at the AIChE 81st National Meetings, Apr 11–14, 1976; in revised form preprinted for NATO Advanced Study Institute on Two-Phase Flows and Heat Transfer, Aug 16–27, 1976, ASI Proceedings, Istanbul, Turkey.
Gidaspow, D., Round Table Discussion (RT-1-2), "Modeling of Two-Phase Flow", 5th International Heat Transfer Conference, Sept 3, Tokyo, Japan, in "Heat Transfer 1974", Vol. VII, pp 163–168, 1974.
Glot, M., Fritte, A., *Prog. Heat Mass Transfer*, **5**, 651–670 (1972).
"Handbook of Natural Gas Engineering", C. F. Bonilla et al., Ed., p 303, McGraw-Hill, New York, N.Y., 1959.
Hariu, O. H., Molstad, M. C., *Ind. Eng. Chem.*, **41**, 1148–60 (1949).
Jackson, R., "Chapter 3. Fluid Mechanical Theory", pp 65–119 in "Fluidization", J. F. Davidson and D. Harrison, Ed., Academic Press, New York, N.Y., 1971.
Jackson, R., *Trans. Inst. Chem. Eng.*, **41**, 13–28 (1963).
Knowlton, T. M., Bachovchin, D. M., *Fluidication Technol.*, **2**, 253–82 (1976).
Lamb, H., "Hydrodynamics", 6th ed, Chapter 6, Dover Publications, New York, N.Y., 1932.
Lax, P. D., *Comm. Pure Appl. Math.*, **11**, 175–94 (1958).
Lyczkowski, R. W., Gidaspow, D., Solbrig, C. W., Hughes, E. D., *Nucl. Sci. Eng.*, **66**, 377–96 (1978).
Mehta, N. C., Smith, J. M., Comings, E. W., *Ind. Eng. Chem.*, **49**, 986–92 (1957).
Nakamura, K., Capes, C. E., *Can. J. Chem. Eng.*, **51**, 39–46 (1973).
Pritchett, J. W., Levine, H. B., Blake, T. R., Gary, S. K., "Numerical Model of Gas Fluidized Beds", 69th AIChE Annual Meeting, Chicago, Nov 1976.
Richardson, J. F., Zaki, W. N., *Trans. Inst. Chem. Eng.*, **32**, 35–53 (1954).
Rowe, P. N., Henwood, G. A., *Trans. Inst. Chem. Eng.*, **39**, 43–54 (1961).
Rudinger, G., Chang, A., *Phys. Fluids*, **7**, 1747–54 (1964).
Shook, C. A., Masliyah, J. H., *Can. J. Chem. Eng.*, **52**, 228–33 (1974).
Soo, S. L., "Fluid Dynamics of Multiphase Systems", p 279, Blaisdell Publishing Co., Waltham, Mass., 1967.
Soo, S. L., *Int. J. Multiphase Flow*, **3**, 79–82 (1976).
Wen, C. Y., Galli, A. F., "Chapter 16, Dilute Phase Systems", in "Fluidization", J. F. Davidson and D. Harrison, Ed., Academic Press, New York, N.Y., 1971.
Yousfi, Y., Gau, G., *Chem. Eng. Sci.*, **29**, 1939–46 (1974).
Zenz, F. A., *Ind. Eng. Chem.*, **41**, 2801–07 (1949).

Received for review March 6, 1978
Accepted December 7, 1978

Partial support for this study was provided to one of the authors (D.G.) by Department of Energy Contract DOE ET-78-G-01-3381.

☆U.S. GOVERNMENT PRINTING OFFICE: 1980-740-145/914